# INVESTIGATING LUNG SOUND-FLOW RELATIONSHIP IN HEALTHY AND ASTHMATIC SUBJECTS IN PRESENCE AND VOID OF HEART SOUNDS

**By**

**IRINA HOSSAIN**

**B.Sc. (Eng.), Bangladesh University of Engineering and Technology, 2000**

**A Thesis Submitted in Partial Fulfillment of the Requirements for the degree of**

**MASTER OF SCIENCE**

**Department of Electrical and Computer Engineering**
**University of Manitoba**

THE UNIVERSITY OF MANITOBA

FACULTY OF GRADUATE STUDIES

*****

COPYRIGHT PERMISSION

# INVESTIGATING LUNG SOUND-FLOW RELATIONSHIP IN HEALTHY AND ASTHMATIC SUBJECTS IN PRESENCE AND VOID OF HEART SOUNDS

BY

IRINA HOSSAIN

A Thesis/Practicum submitted to the Faculty of Graduate Studies of The University of Manitoba in partial fulfillment of the requirement of the degree

Of

MASTER OF SCIENCE

# Abstract

To investigate the relationship between lung sound (LS) and flow, LS signals from 5 healthy adults (Group I), 10 healthy children (Group II) and 7 asthmatic children (Group III) were studied. The LS signals were recorded by an accelerometer placed over right upper lung lobe at different flow rates varied from 0.4 to 3.0 L/s, and the flow signals were measured at mouth. The signals were simultaneously digitized at 10240 Hz. The LS and flow signals were parsed into 100 ms segments with 50% overlap between successive segments. The mean LS amplitude (*mean AMP*) and mean flow (*flow*) were calculated for each segment. The average power ($P_{ave}$) of each segment was calculated from the LS spectrum over different frequency bands between 20-600 Hz. Four different types of models, representing the relationship between *mean AMP* or $P_{ave}$ and *flow*, were investigated using different percentage of flow signal in each inspiratory phase. Results showed a much stronger correlation between $P_{ave}$ and *flow* than *mean AMP* and *flow* for all groups. The best model to describe $P_{ave}$ relationship with *flow* was found to be power relationship in both healthy adults and children groups whereas a third-order polynomial curve best fitted the $P_{ave}$ and *flow* data in asthmatic group. The optimum frequency band to calculate $P_{ave}$ was found to be 150-450 Hz for healthy subjects and 300-600 Hz for asthmatic children. The diminution of heart sound (HS) from LS recordings showed no change in the selected model in all three groups. The results of this study suggest the difference in $P_{ave}$-*flow* relationship in healthy and asthmatic subjects may be used as a diagnostic tool for asthma. In addition, a Wavelet Transform (WT)-based adaptive filtering (AF) was applied to LS signals for heart sounds reduction. Results showed that the WT-based AF reduced heart sounds but also reduced the overall LS average power, and hence altering the original signal of interest. Thus, further investigation on the feasibility of using this method for heart-sound reduction from LS signal is necessary.

# Table of Contents

# List of Figures

# List of Tables

# Acknowledgement

First, I wish to thank Allah for all His blessings and helps.

I would like to express my profound gratitude and appreciation to my supervisor Professor Zahra Moussavi for her continuous support, inspiration and active guidance during this research work. Her critical reviews of the thesis and constructive suggestions were vital to shape my ideas into this dissertation. I have been very fortunate to work in such an affectionate environment under Professor Moussavi whose supervision and mentoring has always been creating a `morality of aspiration' inside me. I would like to acknowledge with gratitude the support from NSERC and University of Manitoba during the course of my gradate studies at University of Manitoba.

My heartiest gratitude to Professor Miroslaw Pawlak for his invaluable help and guidance during the research work. Special thanks to Professor Hans Pasterkamp for his helpful discussions on my research work. I am very grateful to them for serving on my examination committee. A heartiest thanks goes to Professor Jitendra Paliwal for being the external examiner in my oral examination.

I would like to extend my sincere thanks to all of my colleagues and friends here in Winnipeg for their friendship and cooperation. My deepest thanks to my brother and husband for their constant inspiration and support.

# Dedication

To my parents whose unconditional love and blessing is the inspiration of my life.

# CHAPTER 1 – PREAMBLE

**Research Objectives**

- Study lung sound-flow relationship in
  - Healthy children and adults
  - Healthy and asthmatic children
- Investigate lung sound-flow relationship when heart sound is reduced from recorded lung sound
- Evaluate the effectiveness of WT-based adaptive filtering in heart sound removing from lung sound

## 1.1 MOTIVATION

Application of computer technology and digital signal processing techniques in respiratory sound (RS) analysis has proved the use of acoustical analysis of RS as a valuable tool in clinical pulmonary assessment. Computerized RS analysis has shown promise in the diagnosis of upper airway pathologies, respiratory tract infections, swelling, airway edema, malformation and tumor [1-6]. Respiratory acoustical analysis can now quantify changes in lung sounds (LS), make permanent records of the measurements made and produce graphical representations that help with the diagnosis and treatment of patients suffering from lung diseases [7]. Consequently, there is an emergent interest to gather more information of clinical utility from RS and better understanding of the characteristic patterns of these sounds in both patients and healthy individuals. One of the issues of interest for physicians and therefore, researchers in this field is to find a model, which best describes the relationship between respiratory flow and LS of patients compared to that of healthy individuals. Variation in flow rate modifies both the intensity and frequency distribution of the breath sounds [8-10].

Several researchers have studied such relationship between respiratory flow and breath sounds recorded either at trachea or over the chest [10-15]. However, none of them were conclusive to a general model particularly between LS and flow.

Hence, the main motivation of this thesis was to explore the possible models describing the relationship between LS and flow in both healthy individuals and asthmatic patients. The LS was chosen over the tracheal sound due to the more diagnostic value of LS. Determining the pattern of the LS-flow relationship will contribute toward better understanding of the mechanism of breath sound generation as well as better diagnosis of respiratory diseases.

One of the challenges in LS analysis is the interference of heart sounds (HS) with LS as it is an inevitable source of noise that may mask the clinical auscultative interpretation of LS and alters the energy distribution in the spectrum of LS. Removing HS from LS without significantly changing LS is challenging due to their overlap in both time and frequency. Therefore, a simple filtering cannot remove HS from LS. In recent years, the wavelet transform (WT) based denoising techniques have shown effective in many applications including medical signals and images [16]. Since wavelet is a prevailing means of denoising signals, a new adaptive filtering (AF) technique based on wavelet transform has been proposed to remove HS from LS recordings [17]. This method eliminates the need for any reference signal with low computational cost and results in fast and easy implementation. However, the usefulness of the WT-based filter in HS removing was not evaluated with proper frequency domain analysis of filtered signal to compare with that of HS-free LS signal because of the unavailability of pure

HS-free LS signal. In this study, a standard reference was provided to assess the efficacy of the proposed method by doing frequency domain analysis of the filtered signals and HS-free original LS signals extracted manually from the original LS recordings. Furthermore, the LS-flow relationship was investigated for plausible changes as a result of HS removal from LS signals using the manual technique.

## 1.2 BACKGROUND INFORMATION

Breathing is the process by which oxygen in the air is brought into the lungs and in close contact with the blood to carry it to all parts of the body, and carbon dioxide is carried out of the lungs; thus lung can be described as the site of gas exchange. Lung sound is generated by physical process as air turbulence, oscillatory movements of airway walls, abrupt equilibration of gas-compartments with different pressures or gas bubbling through mucus [18]. The generated sound is transmitted to the chest surface through air spaces, parenchyma and chest wall. The parenchyma absorbs the sound, especially the high frequency components, and the propagation speed is very low (25-60 m/sec) [19]. In the airways, sound is propagated through the air (high frequencies) and the airway walls (low frequencies), and the recorded signal is influenced by acoustical impedance mismatch at interfaces, and resonance [19]. Additional unwanted sounds are generated simultaneously, for example by the heart and muscles. The LS generation is affected by lung volume and by the velocity and direction of airflow [20-21] and the intensity is influenced by regional ventilation [22] and closing volume [23]. The LS transmission varies with the individual anatomic variations within the chest cavity [24] and the density of the pulmonary parenchyma affects the propagation and attenuation of sound [25-26].

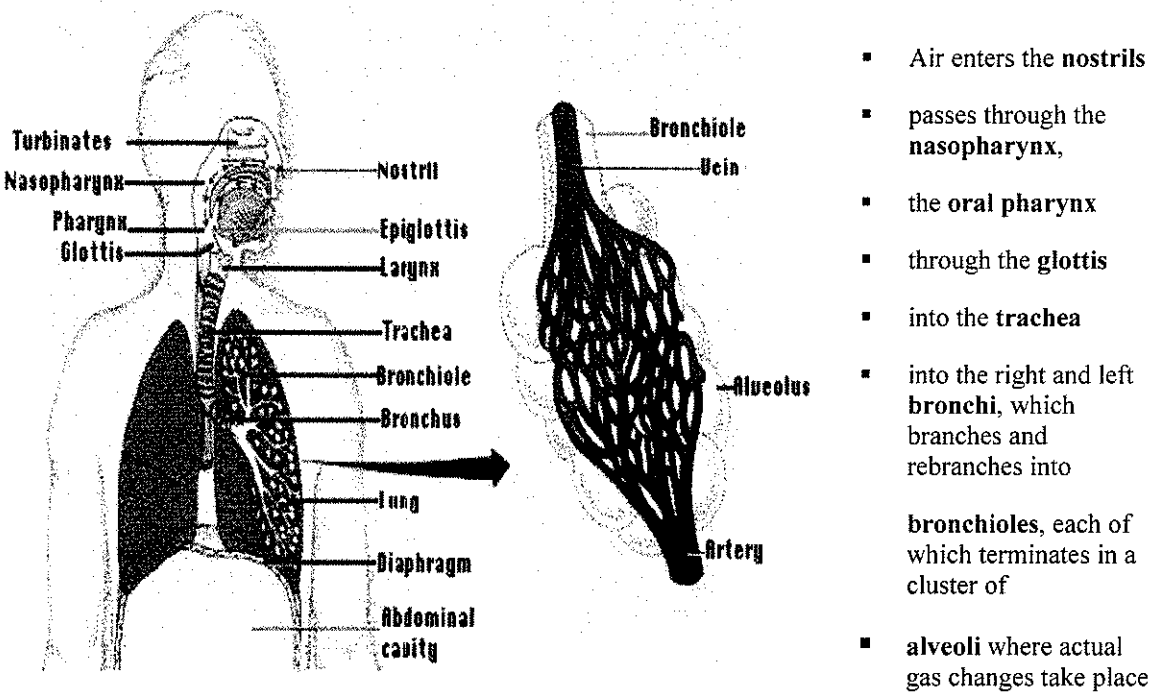


**Figure 1.1.** Anatomy and Physiology of human respiratory system.

The LS amplitude is lower in comparison to the tracheal sound amplitude and is loudest at low frequencies (near 135 Hz) [27], and inspiratory sounds are found to be louder than the expiratory sounds [28]. The effect of lung volume on LS amplitude was found to be less, and the effect was apparent only over the upper lobes [29]. Again, the amplitude differs between persons and different locations on the chest surface [27]. The spectral pattern of normal chest wall breath sound was reported to have an exponential decay of amplitude with increasing frequency and the energy was found to drop off sharply between 100 to 200 Hz, though it could be detected above 1000 Hz with sensitive instrument [12, 20, 27]. It was found that the spectra of infants contained less power below 300 Hz compared with children and adults whereas sound attenuation above 300 Hz was similar in all ages [12]. The frequency spectra of inspiratory and expiratory LS signals are also different. The comparison of inspiratory and expiratory LS average

power at different frequency bands at different flow rates for different locations on the chest showed that inspiratory sounds were louder than the expiratory sounds below 450 Hz, and the highest inspiratory–expiratory (I-E) power difference was in the frequency range of 150-450 Hz [30].

Most common diseases associated with the obstruction to airflow in the respiratory system are asthma, chronic bronchitis, emphysema, cystic fibrosis and sarcoidosis (lower airway obstruction); croup, Laryngotracheobronchitis, Epiglottitis and various tumors and foreign bodies that may involve the upper airway (upper airway obstruction) [18]. Among these, asthma is the most prevalent especially in western countries, which may be due to the changes in the nature of exposure to various factors before birth and during early childhood [18]. Asthma is a chronic inflammatory disorder of the bronchial airways associated with reversible airway obstruction and increased airway responsiveness to a variety of stimuli [18, 31]. The airways react by narrowing or obstructing when they become irritated by allergy, viral respiratory infections, and airborne irritants. This makes it difficult for the air to move in and out. This narrowing or obstruction can cause one or a combination of wheezing, coughing, shortness of breath and chest tightness [18, 31].

Since the invention of *Laënnec's* stethoscope in 1817, physicians use the stethoscope as a routine instrument to listen to RS for clinical diagnosis. However, auscultation with a stethoscope has many limitations [27]. The primary problems in the use and interpretation of stethoscope are physical, physiological, technical and clinical. Auscultation using a stethoscope is very subjective to the individual's interpretation.

External and internal noises may confound sound recognition as pathological or healthy, resulting in possible misdiagnosis. Quantitative measurements or permanent record of an examination is not possible with the use of stethoscope. Consequently, long-term monitoring or correlation of RS with other physiological signals is difficult. Besides, the stethoscope has a frequency response that amplifies frequencies below 112 Hz and attenuates higher frequencies [27]. Acoustic investigations of the lung with computerized methods for the recording and analysis of sounds have overcome many limitations of simple auscultation by stethoscope.

In recent years, the application of digital signal processing and modern computer technology has offered immense advantages for capturing, storage, analysis and communication of RS [7]. There has been a growing interest in respiratory acoustics, as it has shown promise in the investigation of many respiratory diseases. Commonly reported applications of computerized RS analysis are the graphical presentation of important features, permanent records of such features, comparison of data obtained at different times during the progression of respiratory diseases or their treatment, long term monitoring of asthma, monitoring of breathing patterns of infants, monitoring of adults in critical care settings and detection of features and patterns that are not easily recognized by human ear [7]. It may soon be possible to use the RS recordings and analysis to monitor sleep apnea, nocturnal changes of bronchial obstruction in asthma; to assess the response to bronchodilators and to bronchoconstrictors; and to monitor and analyze the bronchial response to inhaled nonspecific bronchoconstrictive agents like methacholine or histamine both in children and adults [32]. With the availability of state-of-the-art acoustical devices, such as air coupled microphones and contact accelerometers that are

more sensitive and specific for respiratory assessment, and various digital signal processing methods, we have entered in the new era of pulmonary assessment by acoustical means.

The problem of background noise is of particular importance in acoustical analysis of RS, which includes any sound not directly associated with respiration. Environmental noises may be avoided by a large degree by recording sound in a room that is free from transient noises or in a body plethysmograph, shielding the sensors with sound isolation materials, and by using suitable sensors [32]. Recently, adaptive digital filtering by computer microprocessor has been effectively applied to further reduce the effect of background noise [33]. However, the reduction of interfering sounds from chest motion, intercostal muscles, skin friction, heart, swallowing, burping, bowl sounds, joint crackles, speech or other noises from the subjects is more intricate to attain without considerably changing the signals that are of interest. Automated artifacts recognition and cancellation may become a built-in and routine part of RS analysis in both clinical and research application [7]. On the other hand, interference of HS with LS, both in time and frequency domains, may not be considered as the background noise, since HS is a regular, quasi-periodic signal. Although different approaches have been proposed to reduce the effect of HS from LS recordings, a preferred signal processing technique has not been established yet so that it can be used in clinical environment. Therefore, one of the objectives of this thesis was to investigate wavelet denoising method to achieve HS reduction from LS recordings.

The relationship between respiratory flow and the amplitude of breath sounds has been under investigation for a number of years. In recent times, a few investigators explored the feasibility of estimating flow from tracheal sound signal using the relationship between flow and tracheal sound [10-14, 34]. The main goal of this study was to investigate the LS-flow relationship, derive a model to describe this relationship and investigate whether the model would change with age or as a result of airway diseases such as asthma. Furthermore, the effect of the presence of HS in the LS-flow relationship pattern by analysis of LS, including and excluding HS, was investigated.

In summary, the objectives of this study were:

- To find a mathematical model that best describes the LS–flow relationship both in children and adults.
- To compare the LS–flow relationship of children with asthma to that of healthy children.
- To investigate the variation of LS–flow relationship when HS are removed from the LS recordings.
- To evaluate the effectiveness of WT-based adaptive filtering technique in HS reduction from LS recordings, both quantitatively and qualitatively.

## 1.3 OUTLINE OF THE THESIS

Subsequent chapters of this thesis are organized as follows:

**Chapter 1** – The purpose of this chapter is to demonstrate the preamble and background information for the thesis. It provides an overview of the anatomy and physiology of

human respiratory system, characteristics of normal LS and common diseases associated with lungs and the problem of interference of noise associated with LS recordings. This chapter defines the research objectives.

**Chapter 2** – This chapter gives a brief review of past research done on LS signals, which comprise studies of LS signal characteristics as well as its relationship with flow, and a short overview of the digital signal processing techniques recommended in the problem of interference cancellation in LS analysis. Each study is discussed with a concise expository of its methodology along with error analysis and performance evaluation if it is available, and the findings that have been reported.

**Chapter 3** – This chapter describes the data acquisition technique and instrumentation used in this research, the signal processing techniques and mathematical models used to determine the LS–flow relationship, and the application of WT-based AF technique to HS removal problem in LS recordings. It represents the detailed data analysis processes for LS–flow relationship modeling and WT-based adaptive filtering of LS.

**Chapter 4** – This chapter summarizes the results of model selection to describe the LS–flow relationship, optimum frequency band to calculate LS average power and the results of data segmentation. It also represents the results of HS reduction from LS recording using WT-based adaptive filtering.

**Chapter 5** – This chapter provides discussions on the results of the current study and summarizes the contributions of the thesis.

**Chapter 6** – This chapter discusses a few directions for possible future works.

# CHAPTER 2 – LITERATURE REVIEW

## 2.1 REVIEW OF RELEVANT RESEARCH PAPERS

Computerized RS analysis has seen major innovations over the past 30 years with rapidly evolving computer technology, data acquisition techniques and state-of-the-art digital signal processing techniques [7]. These techniques have revealed various respiratory acoustic properties related to physiological parameters in various pathological conditions. It has been established that different lung diseases may be diagnosed when adventitious sounds are present, or when patient's LS is perceived as having different features than that of normal LS features. Lung sound studies for diagnostic features include studying its frequency spectra at different locations on the chest [20, 35]; frequency spectra as a function of age and body size [11-12] and lung volume and flow [25]; spectra at different pathological conditions [36-37]; LS amplitude at different locations and as a function of flow [21-22, 24, 28, 37-38]; and the interference of cardiovascular and muscle noises on LS [24, 39]. Recently, extensive interests have originated concerning the airway modeling of human respiratory system that can explain the association between respiratory flow and breath sound quantitatively. The related works exploring the breath sound characteristics and their relationship with respiratory flow are brought up in short in this chapter.

The research on the relationship between LS and flow was launched when experiments discovered that there is a parallel upward shifts of the spectral curve with increasing flow with no changes in the general pattern of the LS spectrum [11]. Other

recent studies revealed that both the mean amplitude and mean frequency of LS are increasing functions of flow [28], although the relation depends on various parameters such as individual's height, weight, age, airway dimension, gas density etc. [27]. As a result, researchers investigated various methods to relate these two signals [9-15, 22-25, 37-38].

In early years, Leblanc and his coworkers [22] studied the relationship between LS amplitude (*AMP*), measured as the peak deflection of a rectified, integrated tracing, and the simultaneously measured inspired flow and volume, and demonstrated a linear relationship between *AMP*, and flow within a wide range of lung volume. Since the points were picked off a chart recorder tracing and the curve fitting was done by eyeballing, the results might not be reliable. Banaszak et al. [37] showed that the logarithm of root mean square (*RMS*) of LS amplitude was linearly related to flow, where they used frequency analysis techniques to analyze LS from 75 to 500 Hz and related the amplitudes to peak of flow measured at mouth. Wooten and his co-workers [38] published a plot of LS *AMP* as a curvilinear function of flow without including actual points where they stated the relation as exponential. Dosani and Kraman [39], and Kraman and Austrheim [24] ascertained that the LS signal was a linear function of the flow above 1.3 *L/s*. They divided the LS intensity by the flow to generate a flow independent measurement and demonstrated that below 1.3 *L/s* the relation was not always linear [39]. In another study, a linear relation between flow and LS *AMP* was suggested [40]. The LS data was recorded from four subjects breathing at functional residual capacity, and peak flow was compared with either the mean or peak LS *AMP*. The linear regression analysis for the peak flow greater than 1.4 *L/s* and the

corresponding mean and peak sound *AMP* showed linear relationship in all subjects. On the other hand, Shykoff and her co-workers reported a good statistical fit between the experimental data and the data estimated from a quadratic model describing the relationship between LS *AMP* and flow [41]. However, the LS envelope used in their study, as an estimate of sound amplitude, had inherent fluctuations that limited the accuracy of assessing a precise power relationship.

Charbonneau et al. [42] used a different equation to relate flow with mean breath sound (both tracheal and lung sound) amplitude (*BSA*) in *Watts* and mean power frequency ($\overline{f}$). However, by *BSA* they meant the area under the spectral curve of LS minus corresponding area under the breath-hold spectra. The model was summarized as

$$\overline{BSA} = A \cdot F / (k\overline{f} - F), \qquad (2.1)$$

where $F$ is flow in *L/s*, $\overline{BSA}$ is mean of *BSA* from the breath sounds recorded at four different locations, $\overline{f}$ is mean power frequency in *Hz*, $A$ and $k$ are constants. Further inspection of this model revealed a nonlinear relationship. According to their model, if $k\overline{f} >> F$, the LS spectral amplitude became linearly dependent on flow. But as flow increased relative to $k\overline{f}$, the relationship became nonlinear with higher dependency on $\overline{BSA}$. They demonstrated that when increasing flow from 0.25 *L/s* to 0.5 *L/s*, $\overline{BSA}$ and flow had a power relationship ($BSA = k \cdot F^{\alpha}$) with $\alpha$ to be approximately 1.6, whereas increasing flow from 0.4 *L/s* to 0.8 *L/s*, $\alpha$ was about 2.

In contrast to all researchers who assumed that a relationship exists between breath sound and airflow, Mussell et al. [35] claimed that both tracheal and lung respiratory sounds were flow independent over the flow range of 1.6-2.6 *L/s*. This result is incongruent with established clinical observations and might be due to some error in their calculation of spectra. For example, some Fast Fourier Transform (FFT) algorithms normalize their output by always assigning a fixed numerical values to the largest point (peak) in the spectrum.

More recently, Gavriely and his co-workers [28] investigated a power relationship between *BSA* and flow, as described by the following equation,

$$BSA = kF^{\alpha}, \tag{2.2}$$

where $F$ is flow in *L/s*, $\alpha$ and $k$ are constants. The amplitude was calculated as the area under the linear spectral curve of breath sounds (calculated over the frequency band of 100-1000 Hz for the LS and 100-2400 Hz for tracheal sound) minus the area under the corresponding spectral curve of breath-hold sounds assuming that these areas correspond to the root mean square amplitude of the sound in time domain. In their studies, lung and tracheal sounds data recorded from six healthy men exhibited the power relationship as stated above and the overall mean±SD (standard deviation) value of the power coefficient ($\alpha$) was determined to be 1.66±0.35. Furthermore, LS power during inspiration was found to be greater than that during expiration, whereas tracheal sound power was independent of respiratory phases. However, neither the mean-square-error (MSE) of the linear regression analysis, nor the correlation coefficient between log (*BSA*) and log($F$) were reported in their study.

The existence of a relationship between RS and flow, encouraged several researchers to try estimating flow from RS mainly from tracheal sounds. Making use of the different signal characteristics, Soufflet et al. [10] estimated flow from tracheal sounds with eight methods divided into two groups of four. For the first group of experiments, they assumed that a relationship existed between flow and various tracheal signal parameters (mean amplitude of sound (in time-domain), mean amplitude of spectrum, mean frequency of spectrum and the product of mean amplitude and mean frequency) and was thus reflected by the variation of certain parameters. Four different parameters were tested and for each parameter $P$, a specific reference curve representing the variation of $P$ versus flow was derived for each subject and the unknown flow was estimated from the calculated $P$ and reference curve. In the second group, a hierarchical clustering analysis of sound spectra was made for revealing the frequency modifications induced by the flow where each cluster is associated with a reference flow and reference spectrum. Their results showed a mean uncertainty of about 15% between actual and estimated flow for all the eight methods except one.

Que et al. [34] estimated tracheal flow from tracheal sounds by using linear relationship between flow and sound in both patients (patients with unstable airway obstruction and patients with stable asthma) and normal subjects. Flow and tracheal sounds were measured simultaneously during two separate 30-sec intervals. For one 30-sec period the relationship between flow and sound was determined and this relationship was used to derive flow and volume from the amplitude of the sound signal of the second measurement period. The accuracy of measurement was assessed by comparing the volume obtained from integration of the measured flow ($Vm$) to the volume estimated

from the sound signal ($Ve$) and the mean difference between $Ve$ and $Vm$ was shown to be $0.009\pm0.046$ $L$. Lately, Yap and Moussavi [14] explored several possible relationships between flow ($F$) and tracheal sound average power ($P_{ave}$) over different frequency bands. Experiments with three models (linear ($P_{ave}= kF$), power ($P_{ave} = kF^{\alpha}$) and exponential ($P_{ave} = ke^{F\alpha}$) relationship model) showed that the relationship between $F$ and tracheal $P_{ave}$ could be best represented by an exponential model. For that reason, the exponential model was used to estimate flow. The results showed that the estimated flow followed actual flow well with an error of $5.8\pm3.0$ %

A non-invasive acoustical method has been developed to detect respiratory phases (inspiration/expiration) without direct measurement of flow with 100% accuracy [30]. In that method, onsets of breaths were detected using tracheal sound signal and the respiratory phases (inspiration and expiration) were identified from the LS signal. Most recently, Hossain and Moussavi [15] estimated respiratory flow from LS average power determining a piecewise linear model between flow and LS average power. The results showed an overall estimation error of $10.2\pm3.3$%.

The correlation between LS alterations and airways obstruction in asthma has long been recognized in clinical practice, although the precise pathophysiological mechanisms of this relationship have not been determined. Tinkelman et al. [43] used computer analysis of breath sounds to measure sound intensity levels in both healthy and asthmatic children. The intensity levels were derived using a microcomputer-based program that digitized audio signals and calculated energy values at every 25-ms interval throughout each signal. Results showed that there were statistical differences between

mean intensity levels for LS in healthy children between 2 and 6 years and the mean intensity levels for wheezing sounds in the same age group, as well as wheezing sounds in asthmatic patients over the age of 8 years ($p < 0.002$). It is being assumed that airway narrowing in asthma, either spontaneous or induced by bronchial provocation, will increase the flow required to generate inspiratory breath sounds and will change the relation of flow and LS intensity. Therefore, in this study the LS-flow relation was investigated profoundly for both healthy and asthmatic cases using different mathematical models.

In LS analysis, the reduction of interfering sound from intercostal muscles, chest wall movement and the heart is challenging to achieve without significantly disturbing the waveforms that are of interests. Although the effects of ambient noise could be considerably reduced by using a sound proof room and suitable accelerometer, the removal of heart noise interference is complicated since they overlap both temporally and spectrally [20]. In addition, frequency contents could change or exhibit a shift due to several factors such as the inherent variability of biological system, conditions during signal acquisition, and cardiac disorder. The time variance, nonlinearity, and transmission changes of the systems involved exclude direct subtraction of separately recorded heart sounds from the contaminated LS as a solution. High-pass filtering (HPF) with cut-off frequency below some compromised and arbitrary value in the range between 70-100 Hz has conservatively been used to diminish this interference [44]. However, the problem of using HPF is – low frequency HS as well as LS are suppressed, but higher spectral components of HS may still contaminate the LS signal [20]. An alternative approach proposed for HS removal was the selective sound analysis during parts of the cardiac

cycle that are free of HS (diastole) known as "ECG-gating" [45]. This method is limited by the number of samples due to the selective sampling of the sound signal and it needs an extra recording of ECG signal.

The application of least-mean-square (LMS) AF technique was suggested to overcome this problem by several researchers [46-48]. However, the overall HS reduction by these LMS-AF methods was moderate (50%-80%, 24%-49% and 75%-83%, respectively) and none of the methods has led to a gold-standard or superior method to resolve the problem of HS reduction in LS recordings.

A reduced order Kalman filtering (ROKF) was applied to this problem where an autoregressive (AR) model was fitted to the HS signal manually extracted from portions of recordings without LS [49]. The state-space equations necessary for the ROKF were set up assuming LS signal as a colored additive process in the observation equation. Although this method eliminated the necessity of time alignment required by LMS-AF method, the computational complexity of the algorithm was very high and all the results mentioned were based on synthesized signals, not true LS recordings.

Recursive least squares (RLS) filtering algorithm was used for HS reduction in LS recordings by Lu et al. [50] where the filter order was about 8 times lower than that in the ROKF-RLS study mentioned above. Their RLS method was applied in real-time, requiring a separate HS recording simultaneously with the LS acquisition. The HS signals were band-pass filtered between 20-100 Hz, a range that may include LS and excludes HS at higher frequencies.

An adaptive heart-noise reduction method, based on fourth-order statistics (FOS) of the recorded signal was proposed by Hadjileontiadis and Panas [51]. Using a single sound recording, they tried to obtain all signals needed for AF with small number of taps. The Localized Reference Estimation (LOREE) algorithm was developed for HS locations using band-pass filtering and thresholding. After complex signal processing, improved results were obtained over LMS adaptive filtering and HPF, but the method was more computationally intensive and proper quantitative comparison was not done to evaluate the performance of the algorithm.

The discrete wavelet transform was used to achieve alignment of input and reference signals for successive adaptive separation of HS from LS with a block fast transversal filter (BFTF) AF algorithm [52]. The main objective of these investigators was the development of time delay estimation scheme and its comparison with a cross-correlation method for HS localization in LS recordings. The LS recordings were separated into subbands using WT for the application of the time delay estimations, and were reconstructed after application of AF per subband. A formal qualitative assessment of the possible alteration of LS was not reported in their study.

A WT-based AF technique has been proposed for de-noising LS signal from HS [17]. An adaptive separation of desired signal from the unwanted signal was achieved through an iterative wavelet decomposition-reconstruction process based on hard thresholding of the WT coefficients at every iteration. HS appeared to be well reduced in the time and frequency domain relative to the signals after HPF and to the original signals. This method also eliminated the need of any reference signal with low

computational cost, and fast and easy implementation. Again, HPF was used as the main method of comparison and the qualitative assessment of the filtered signal was not exhibited.

Very recently, RLS adaptive noise cancellation (ANC) filtering has been applied to six recorded LS data from healthy subjects for reducing HS in LS recordings [53]. The reference input for the RLS-ANC filter was derived from a modified band-pass filtered version of the original signal. The algorithm was designed to have infinite memory ($\lambda = 1$) and low order ($M = 2$) to adequately track all of the variations in second order statistics of both LS and HS signals. The comparison between the power spectral density (PSD) of original LS segments, with and without HS, and the corresponding RLS-ANC filtered LS segments has shown effectiveness of the RLS filtering method to reduce HS from LS recordings with minimal distortion of LS. However, the processing time of the method is substantial, with at least a ten-fold increase in time for the RLS-ANC over the WT-based AF technique proposed in [17].

Nonetheless, none of the above methods except one [53] were being evaluated quantitatively due to the non-availability of the pure LS signal. Consequently, the evaluation of the WT-based AF [17] was done qualitatively without proper frequency domain analysis of the filtered signal compared to pure LS signal. In order to quantitatively assess the effectiveness of WT-based AF, a HS-free LS reference was extracted from LS recordings manually. The average PSD of HS-free original LS signal, and filtered LS signal was compared in different frequency bands. Finally, the qualitative evaluation was done by listening to the original and filtered signal by experts.

## 2.2 SUMMARY

A brief overview of significant research works accomplished in finding the relationship between LS and flow in patients and healthy subjects, and different proposed HS reduction techniques from LS have been presented. The methodology used in each study was discussed along with their effectiveness and limitations. The findings of each study were summarized in brief.

# CHAPTER 3 – MATERIALS AND METHODS

## 3.1 SUBJECTS, INSTRUMENTATION AND DATA ACQUISITION

Data from twenty two subjects, participated in three different studies previously conducted at the Respiratory Acoustics Laboratory, Manitoba Institute of Child Health (Director: Prof. H. Pasterkamp) were accessed for this project. All the subjects were non-smokers and they were divided into three groups: 5 healthy adults (2 males) aged 25±0.84 (mean±SD) years (Group I), 10 healthy children (7 males) aged 10±3 years (Group II), and 7 asthmatic children (4 males) aged 11±3 years (Group III). The recordings were done in the Respiratory Acoustics Laboratory, University of Manitoba. Informed consent was obtained from the participants and/or their parents (guardian) before recording LS data. Physical characteristics of subjects participated in this study are given in Table 3.1.

LS data of each subject had been recorded using a piezoelectric accelerometer (Siemens EMT25C) placed at the 3$^{rd}$ intercostal space right midclavicular area (right upper lung lobe or RUL) by double sided adhesive tape rings. Three LS recordings from each subject of Group I was obtained at target flow rates of 0.5 L/s (low), 1.0 L/s (medium) and 1.5 L/s (high). Each recording was consisted of 50-second target flow breathing followed by a 10-second breath-hold to measure the background noise. Data of Group II was obtained from a previous research done for acoustical respiratory phase detection without airflow measurement [30], in which healthy children were asked to breathe at different flow rates from low (0 – 0.4 L/s) to high (0.8 – 1.2 L/s) in a single

recording. They breathed at the target flow rate consistently for a minimum of five complete breaths at each level, followed by a 5-second breath-hold as the reference for background noise. The LS data of asthmatic subjects were accumulated from the respiratory acoustic laboratory, University of Manitoba data archive. Data were collected from children, while they were being treated for asthma at the Winnipeg Children

| Subject No. | Age (yr) | Height (cm) | Weight (kg) | Gender |
|---|---|---|---|---|
| **Healthy Adults (Group I)** | | | | |
| 1 | 26 | 175 | 70 | M |
| 2 | 25 | 180 | 80 | M |
| 3 | 26 | 164 | 62 | F |
| 4 | 25 | 170 | 64 | F |
| 5 | 24 | 162 | 54 | F |
| **Healthy Children (Group II)** | | | | |
| 1 | 10 | 141 | 35 | M |
| 2 | 4 | 63 | 20 | M |
| 3 | 9 | 64 | 36 | M |
| 4 | 13 | 79 | 50 | M |
| 5 | 11 | 76 | 42 | M |
| 6 | 7 | 69 | 32 | M |
| 7 | 11 | 72 | 36 | F |
| 8 | 11 | 78 | 44 | F |
| 9 | 7 | 68 | 30 | M |
| 10 | 10 | 73 | 34 | F |
| **Asthmatic Children (Group III)** | | | | |
| 1 | 12 | 167 | 51 | F |
| 2 | 12 | 137.6 | 32 | M |
| 3 | 15 | 171 | 32 | M |
| 4 | 7 | 125 | 27 | M |
| 5 | 11 | 143 | 32 | M |
| 6 | 7 | 131 | 41 | F |
| 7 | 13 | 153 | 39 | F |

**Table 3.1.** Physical characteristics of study subjects.

HOSPITAL. LS DATA WERE RECORDED IN A SINGLE RECORDING OF 32±7 S INCLUDING 5-SECOND BREATH-HOLD AT THE END OF EACH RECORDING AND EACH SUBJECT BREATHED AT DIFFERENT TARGET FLOW RATES VARIED FROM 0.4 L/S TO 1.3

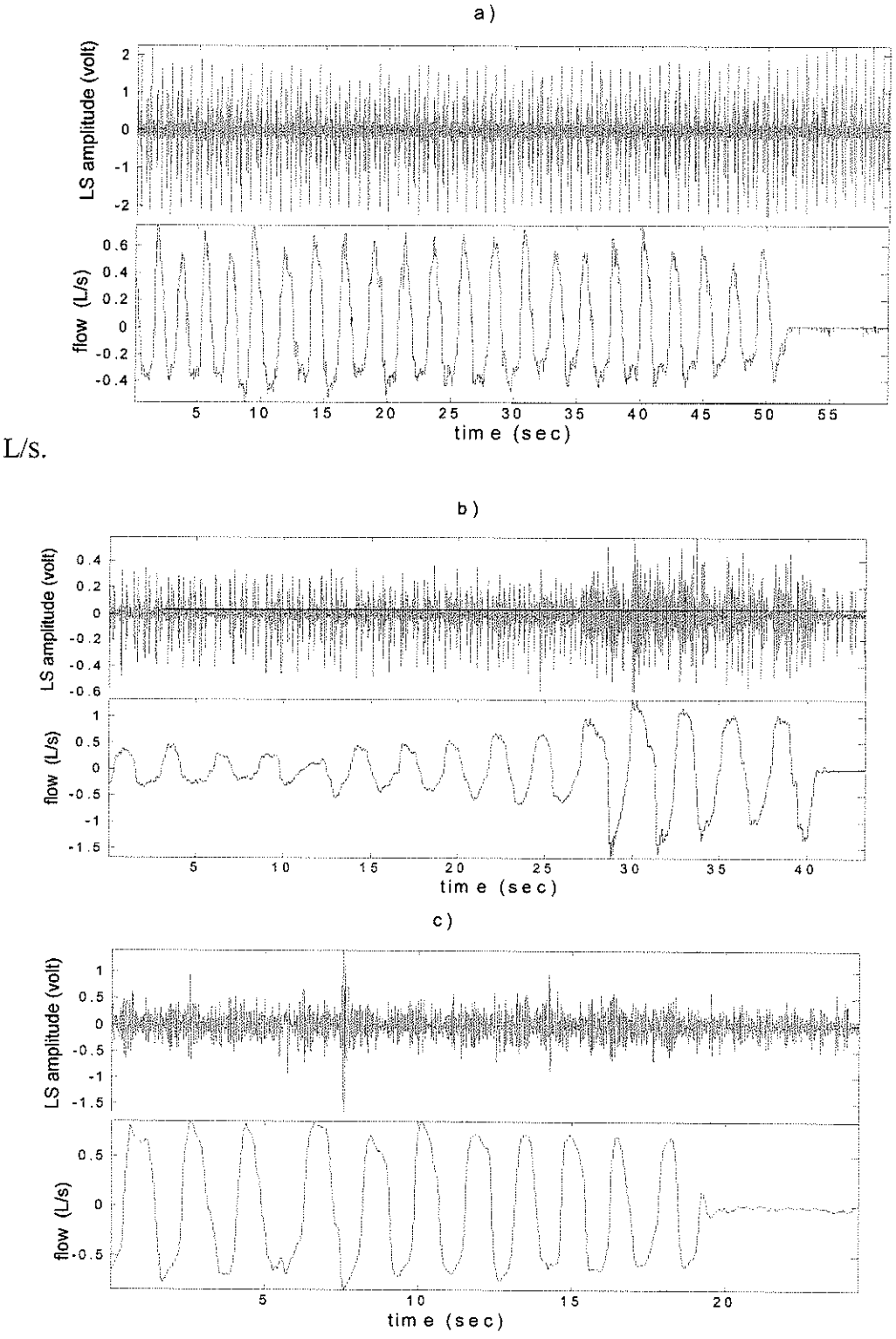


L/s.

**Figure 3.1.** Examples of recorded lung sound and flow signals:

a) Group I b) Group II c) Group III.

The LS signals of all groups were band-pass filtered in hardware using a custom-built eighth order Butterworth filter with the pass-band 50–2500 Hz and amplified by gain of 200. With a nose clip in place, flow signals were recorded concurrently with a mouthpiece attached to a calibrated pneumotachograph (Fleisch #3). All signals were digitized at the 10240 Hz sampling rate and 12 bits per sample (National Instruments DAQ). The flow signals were later decimated to 320 Hz. Subjects maintained target flow levels by monitoring and modifying their breathing while observing flow and volume targets on a computer (custom written application in LabVIEW®, National Instruments). Figure 3.1 illustrates the recorded LS signals and flow signals for each study group.

## 3.2 METHODOLOGY

### 3.2.1 LUNG SOUND AND FLOW RELATIONSHIP MODELING

#### 3.2.1.1 Artifact Removal and Data Segmentation

The first part of data analysis consisted of artifact removal. Artifacts from swallowing, burping, speech or other noises from the subjects were removed from all the sound recordings including breath-hold. Artifact segments were identified manually by visual (from spectrogram) and auditory (listening) means and were marked for exclusion from further analysis.

The presence of HS in time domain signals can easily be identified manually from the spectrogram of the original LS signal as the segments with HS shows higher power at low frequencies (Figure 3.2), and by listening to the signal in time domain.

Hence, the HS-free segments of LS signals were obtained manually by visual and auditory means.

It is known that there is a threshold flow, which needs to be exceeded in order for breath sound to be recognized, and at low flow rates the breath sound amplitude does not exceed the background noise [10, 34]. Hence, there might be a range of flow where

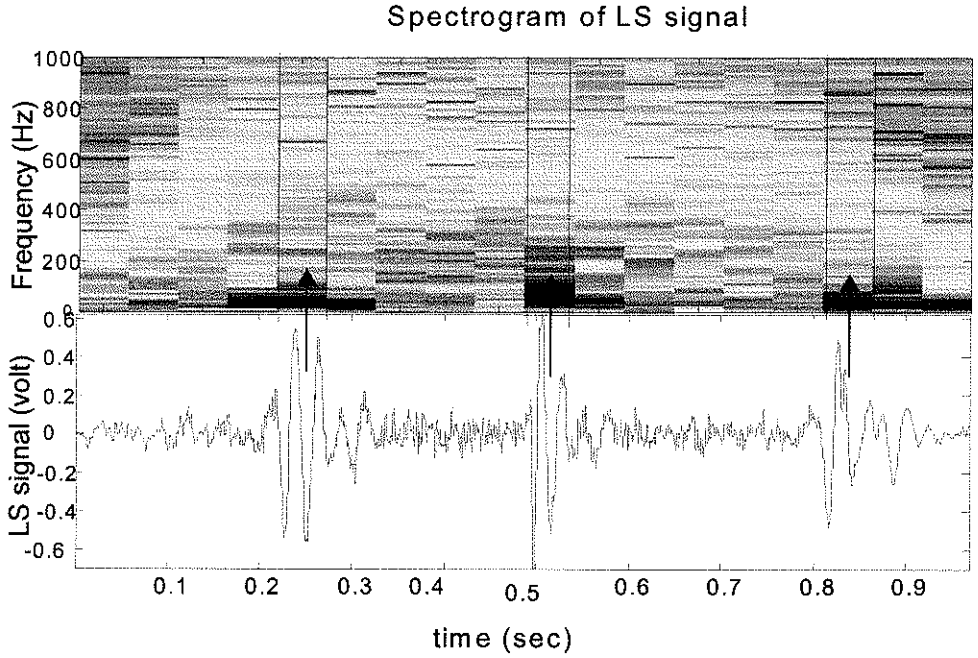


**Figure 3.2.** Example of accumulating HS-free segments of lung sound signal.

no relationship between breath sound and flow could be obtained. Moreover, the relationship might change as the flow increases from zero to the target level. Taking these facts into consideration, the relationship was examined for different percentage of inspiratory flow. Hence, the flow-gating consisted of segmentation of the flow signal as upper X% of each inspiration, where X was varied from 10 to 100 with increment of 10 and the corresponding LS signals were utilized for analysis (Figure 3.3). The goal was to investigate the LS-flow relationship when different percentage of inspiration was taken into account. The breath hold signals were sequestered as including and excluding HS

with the same procedure. The breath-hold segments excluding HS were used as an estimation of background noise [32, 54 ].

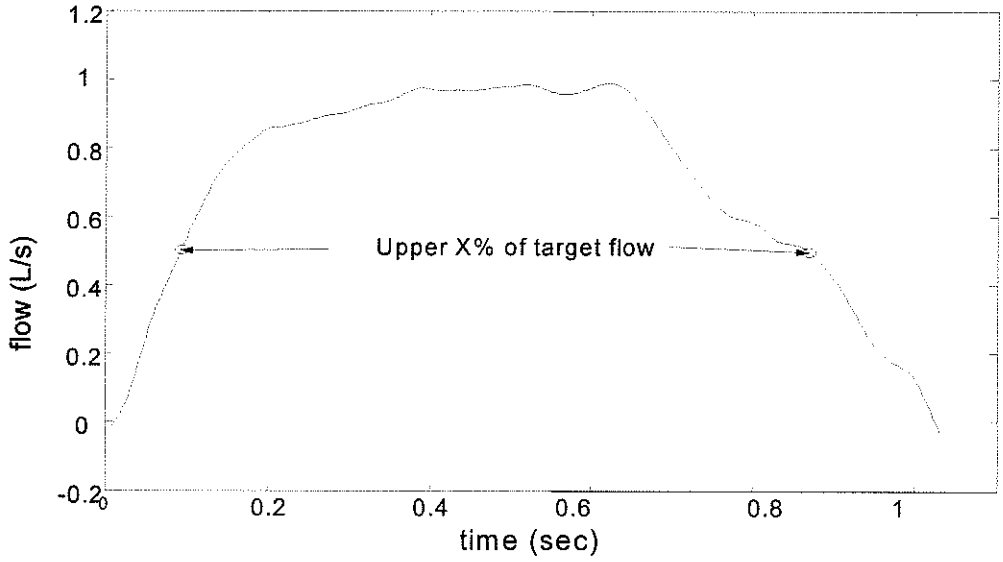


**Figure 3.3.** Flow signal segmentation as upper X% of each inspiration.

### 3.2.1.2 Mean flow and mean Lung sound Amplitude Calculation

In order to obtain the mean LS amplitude (*mean AMP*) the Hilbert Transform of the corresponding flow-gated sound segments was computed. Hilbert Transform of a real valued signal *x(t)* is defined as

$$y(t) = \mathrm{H}_x(t) = \frac{1}{\pi}\int_{-\infty}^{\infty}\frac{x(\tau)}{\tau - t}d\tau, \tag{3.1}$$

where the principal value of the integral is used. Hilbert Transform introduces a phase shift of -π/2 at each positive frequency and +π/2 at each negative frequency. When a real signal *x(t)* and it's Hilbert Transform $y(t) = \mathrm{H}_x(t)$ are used to form a new complex signal $z(t) = x(t) + jy(t)$, the signal *z(t)* is the "analytic signal" corresponding to the real signal *x(t)* with all "negative frequencies" of *x(t)* being filtered out [55-56]. Since *z(t)* has

the same amplitude and frequency content as the original real data, it is useful in calculating instantaneous attributes of a time series, especially the amplitude and frequency. The instantaneous amplitude is the amplitude of the complex Hilbert transformed signal *z(t)*, and the instantaneous frequency is the time rate of change of the instantaneous phase angle. Due to its simplicity, Hilbert Transform is a very popular method for envelope detection of time varying signals. The resulting LS envelope after Hilbert Transform is illustrated in Figure 3.4. The envelope of Hilbert Transformed sound segments was sequestered into 1024 data samples (100 ms) and 50% overlap between consecutive segments and the average was calculated afterward to get the *mean AMP* of the LS segments. The mean flow (*flow*) was also calculated simultaneously for every segment (Figure 3.4).

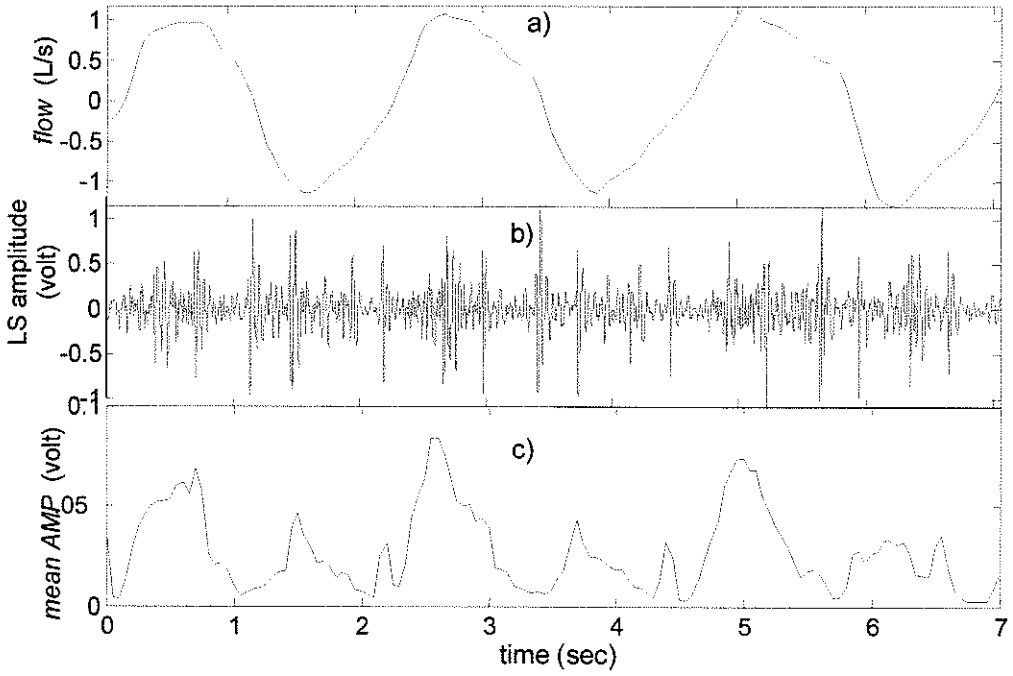

**Figure 3.4.** Calculated mean flow (*flow*) and mean LS amplitude (*mean AMP*) for every 100 ms segment of a LS signal recorded from a typical subject: a) Mean flow (*flow*) b) Original LS signal c) Mean sound envelope (*mean AMP*) calculated after Hilbert Transform of original LS signal.

#### 3.2.1.3 Average Power Computation of Lung Sound signal

The flow-gated and both HS-contaminated and HS-free LS sections of the lung sound recordings were divided into 100 ms (1024-sample) segments using Hanning window, with 50% overlap between successive segments. The power spectrum of each segment was calculated using FFT and averaged over the inspiratory segments to get the average power spectrum density (PSD). The average PSD of breath-hold segments was also calculated in similar fashion and was subtracted from the average PSD of LS segments to eliminate the effect of background noise in the analysis. The average spectra

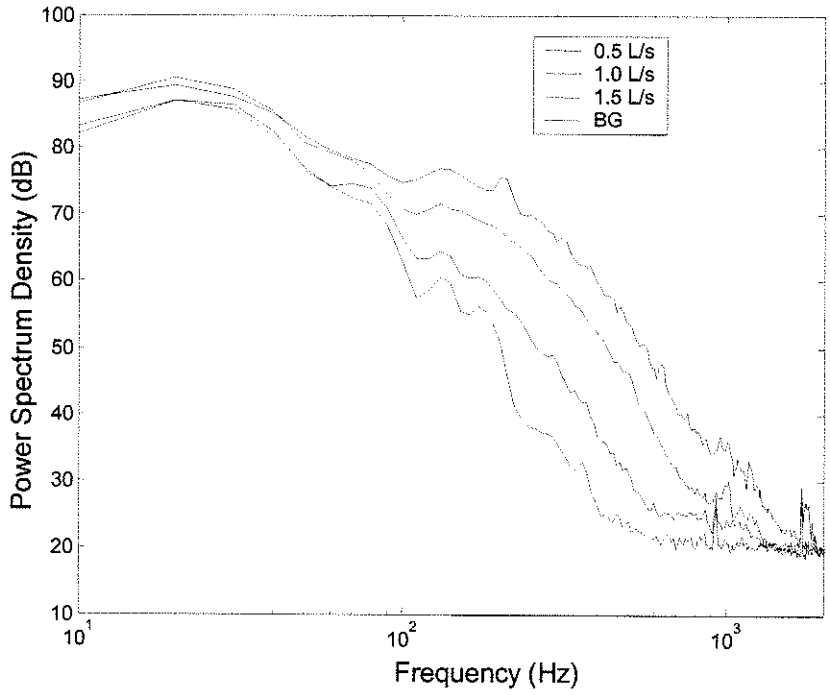


**Figure 3.5.** The Power Spectrum Density (PSD) of LS signal at different flow rates for a typical subject.

of LS segments at different flow rates and breath-hold segments are shown in Figure 3.5 for a typical subject. Since it is noted that increasing flow causes upward shift of spectral curve with no change in the shape, a frequency band was tried to determine where the average power of LS ($P_{ave}$) had the highest correlation with the flow signal. Hence, the $P_{ave}$ of LS signals were calculated over the octave frequency bands: 20-40 Hz, 40-70 Hz, 70-150 Hz, 150-300 Hz, 300-600 Hz, as well as some other frequency bands: 70-300 Hz, 70-450 Hz, 100-300 Hz, 100-450 Hz and 150-450 Hz. Figure 3.6 illustrates an example of calculated average power of a recorded LS signal from it's spectrogram.

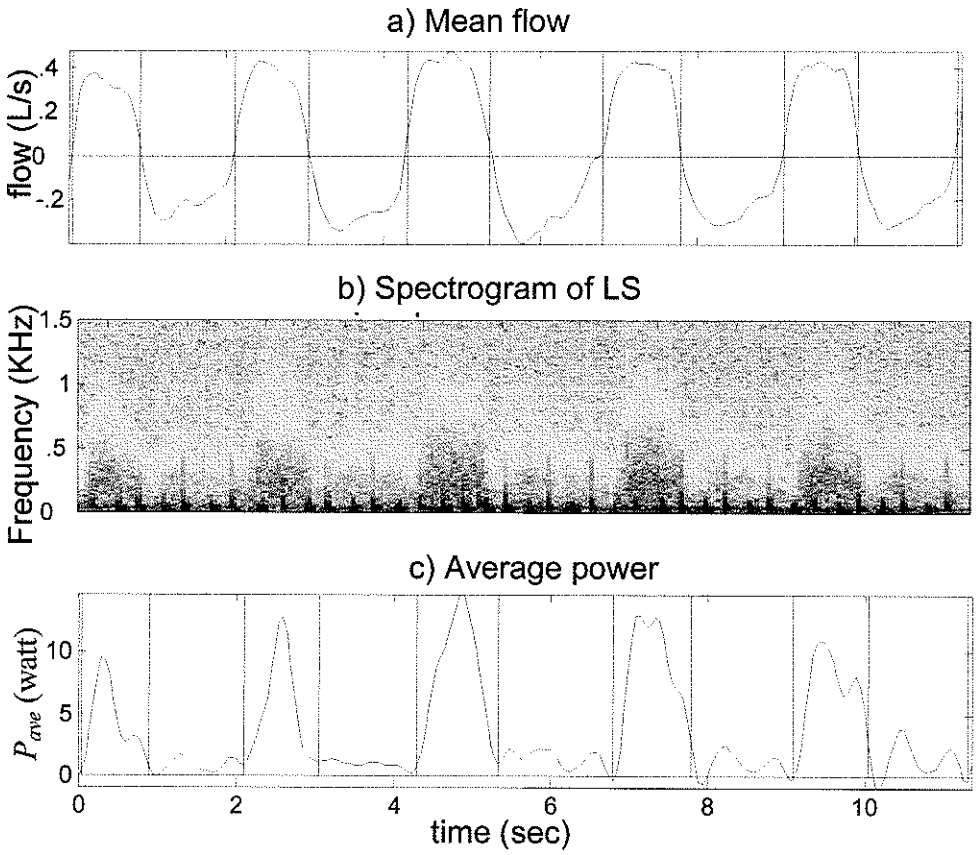


**Figure 3.6.** The spectrogram of a typical LS signal and the average power calculated at 150-450 Hz frequency band.

#### 3.2.1.4 Modeling the relationship between Lung sound and Flow

The following four models describing the relationship between either *mean AMP* or $P_{ave}$ and *flow* were investigated:

1) Power relationship between *mean AMP* and *flow*:

$$mean\ \ AMP \ \propto \ flow^{\,k} \ \rightarrow \log(\ mean\ \ AMP\ ) \propto k \log(\ flow\ ),\ \ k = 1,2,3$$

2) Exponential relationship between $P_{ave}$ and *flow*:

$$P_{ave} \ \propto \ e^{\,\beta\ flow} \qquad \rightarrow \log(P_{ave}) \propto \beta\ flow$$

3) Power relationship between $P_{ave}$ and *flow*:

$$P_{ave} \ \propto \ flow^{\ \alpha} \ \rightarrow \log(\ P_{ave}\ ) \propto \alpha\ \log(\ \ flow\ \ )$$

4) 2nd and 3rd degree polynomial relationship between $P_{ave}$ and *flow*:

$$P_{ave} = k_1 flow^2 + k_2 flow + k_3 \text{ and } P_{ave} = k_1 flow^3 + k_2 flow^2 + k_3 flow + k_4$$

where $\alpha$, $\beta$, $k_1$, $k_2$, $k_3$ and $k_4$ are constants. All the LS features, *mean AMP*, $P_{ave}$ and $\log(P_{ave})$, were normalized dividing by their maximum values.

#### 3.2.1.5 Selection of Optimum Model

In order to find an appropriate model that best describes the LS-flow relationship, the model coefficients of the model 1 to model 3 were derived by using linear regression analysis which fitted a straight line to the measurements done for the model variables in least square sense. Besides, the correlation coefficient ($r$) between the regression line and the actual data was computed which quantifies the degree of linear association between the two variables (Table 3.2). The model that acquired the highest $r$ with least mean-square-error (MSE) between the regression line and the actual data was

chosen as the right most model. In addition, a polynomial curve of order two and order three (model 4) were fitted to the $P_{ave}$–*flow* data to find the best fit curve in least square sense. The values of $r$ between the experimental data and the data estimated from model coefficients were also calculated.

| Correlation Coefficient value ($r$) | Direction and strength of Correlation |
|---|---|
| -1 | Perfectly negative |
| -0.8 | Strongly negative |
| -0.5 | Moderately negative |
| -0.2 | Weakly negative |
| 0 | No association |
| 0.2 | Weakly positive |
| 0.5 | Moderately positive |
| 0.8 | Strongly positive |
| 1 | Perfectly positive |

Note.—The sign of the correlation coefficient (ie, positive or negative) defines the direction of the relationship. The absolute value indicates the strength of the correlation.

**Table 3.2.**[1] Interpretation of correlation coefficient.

[1]Kelly H. Zou, Kemal Tuncali, Stuart G. Silverman, Correlation and Simple Linear Regression. *Radiology* 2003; 227:617–628.

#### 3.2.1.6 Synopsis of LS-flow relationship Modeling

The detail process flow of LS-flow relationship modeling was summarized in the following Data Analysis Flow Chart (Figure 3.7). Data from each subject was analyzed separately so that each model had its own parameters ($r$ and MSE) for each subject and later the parameter values were averaged among the subjects for each model.

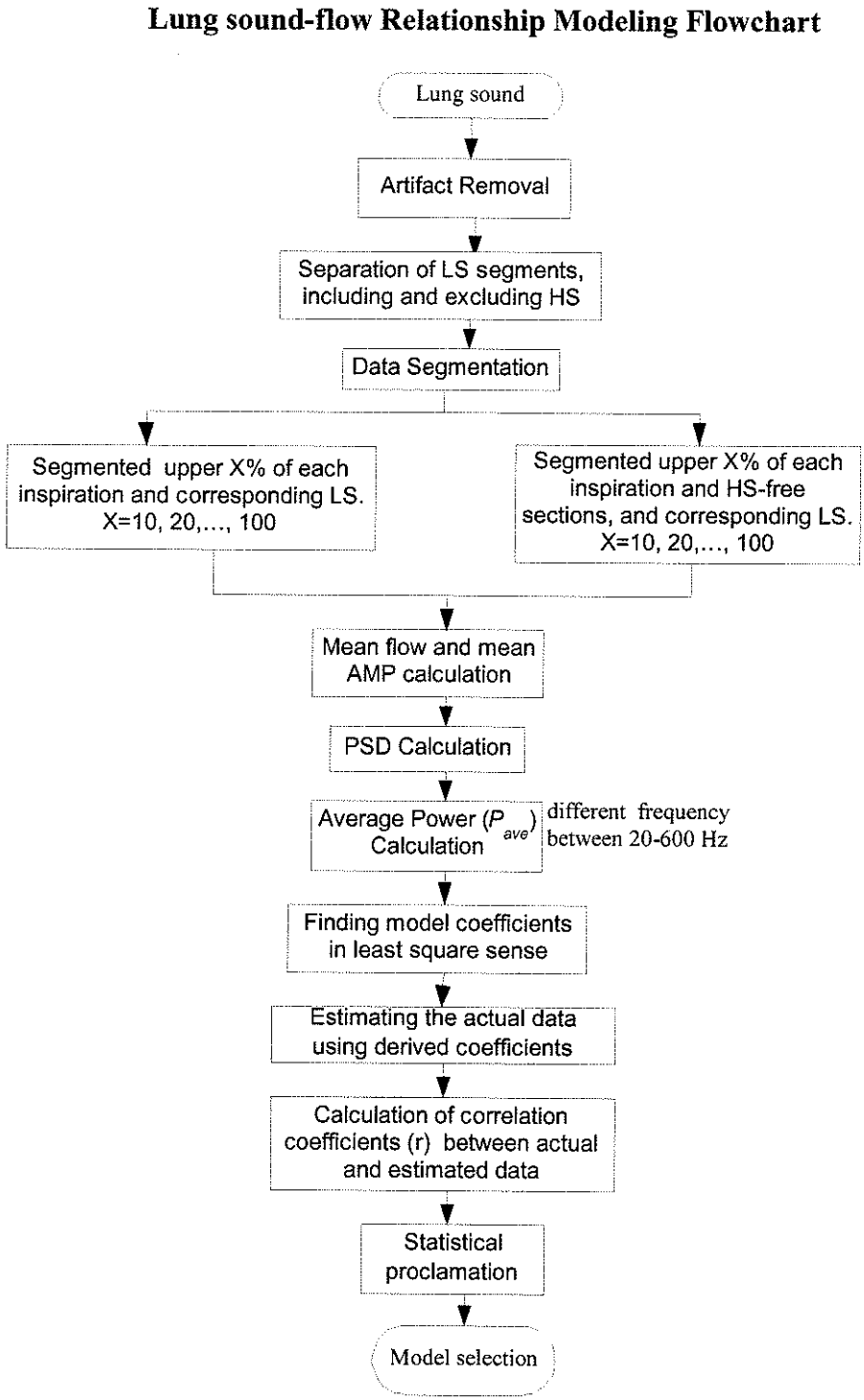


**Figure 3.7.** Data analysis flowchart for LS-flow relationship modeling.

### 3.2.2 HEART-NOISE REDUCTION OF LS USING WT-BASED ADAPTIVE FILTERING

#### 3.2.2.1 Wavelet Analysis

**I. The Continuous Wavelet Transform**

A wavelet is a waveform of limited duration that has an average value of zero and a defined function $\psi(t)$ [57]. Some examples of wavelets commonly used in signal processing are shown in Figure 3.8. By dilation, or changes of scale (s), and translations, i.e., time domain window regions of size τ, families of wavelets are formed based on the main or "mother" wavelet,

$$\psi_{s,\tau}(t) = \frac{1}{\sqrt{s}}\psi\left(\frac{t-\tau}{s}\right), \qquad s > 0, \tau \in \Re \tag{3.2}$$

where s is the dilation parameter and τ is the translation parameter [58].

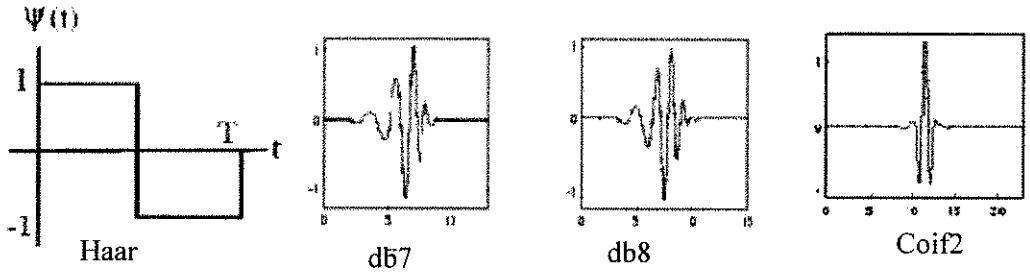


**Figure 3.8.** Examples of some commonly used wavelets.

The continuous wavelet transform (CWT) of a 1-D function $f(t) \in L^2(\Re)$, $L^2(\Re)$ is the vector space of measurable, square integrable function $f(t)$, is defined in a Hilbert space, as the projection of the function onto the wavelet set $\psi_{s,\tau}(t)$ [57]:

$$CWT_f^{\psi}(\tau, f) = \Psi_f^{\psi}(\tau, s) = \frac{1}{\sqrt{|s|}}\int f(t)\psi^*\left(\frac{t-\tau}{s}\right)dt \tag{3.3}$$

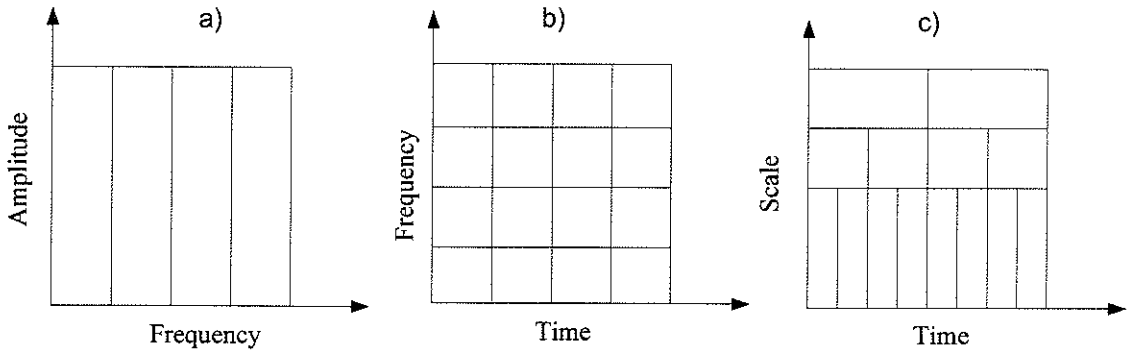


**Figure 3.9.** Comparison of a signal represented in different domains with a) FT representation b) STFT representation c) WT representation.

The scale, $s$ of the wavelet can be considered as the inverse of frequency. Larger scales correspond to dilated signals and small scales correspond to compressed signals. Unlike the Short Time Fourier Transform (STFT) which has a constant resolution at all times and frequencies, the wavelet transform (WT) has a good time and poor frequency resolution at high frequencies, and good frequency and poor time resolution at low frequencies (Figure 3.9). This approach is known as "Multiresolution Analysis (MRA)". The reconstruction of the function is possible using the following formula:

$$f(t) = \frac{1}{c_\psi^2} \int_s \int_\tau \Psi_f^\psi(\tau, s) \frac{1}{s^2} \left( \frac{t-\tau}{s} \right) d\tau \, ds, \tag{3.4}$$

where $c_\psi^2$ is the "admissibility constant" depends on the wavelet used and satisfies the following "admissibility condition":

$$c_\psi = \left\{ 2\pi \int_{-\infty}^{\infty} \frac{|\hat{\psi}(\omega)|^2}{|\omega|} \right\}^{\frac{1}{2}} d\omega \quad < \quad \infty \tag{3.5}$$

where $\hat{\psi}(\omega)$ is the Fourier Transform of $\psi(t)$.

The CWT is particularly good at exhibiting signal information in great detail; however, due to limited computational power available in computer systems, it is necessary to discretize the transform.

## II. Multiresolution Analysis: The Discrete Wavelet Transform

The discrete wavelet transform (DWT) calculates the wavelet coefficients at discrete intervals of time and scale, instead of at all scales. Therefore, it requires much less computation time than the CWT without much loss of detail. With the DWT a fast algorithm is possible which makes use of the fact that if scales and positions are chosen based on power of two (dyadic scales and positions), the analysis is very efficient. The scheme is known as "subband coding".

The wavelet multiresolution analysis is based on the scaling function $\phi(t)$ and a chain of closed, linear "approximation" spaces, $\mathbf{V}_j$ such that $\ldots\mathbf{V}_2 \subset \mathbf{V}_1 \subset \mathbf{V}_0 \subset \mathbf{V}_{-1} \subset \mathbf{V}_{-2}\ldots$ and satisfy some specific properties [58-59]. By dilation and translation of the scaling function and the mother wavelet the following functions are derived:

$$\phi_{j,k}(t) = 2^{\frac{-j}{2}}\phi(2^{-j}t-k), \text{and} \quad \psi_{j,k}(t) = 2^{\frac{-j}{2}}\psi(2^{-j}t-k), \quad j,k = 1, 2, \cdots, J \in \mathrm{Z} \tag{3.6}$$

where $j$ represents the scale or corresponding resolution of the functions and $k$ localizes the functions in time. On each $j$ the function $\phi_{j,k}(t)$ forms an orthonormal basis for $\mathbf{V}_j$ and $\psi_{j,k}(t)$ forms an orthonormal basis for $\mathbf{O}_j$, where $\mathbf{O}_j$ is the orthogonal complement of $\mathbf{V}_j$ in $\mathbf{V}_{j-1}$ defined as:

$$\mathbf{V}_{j-1} = \mathbf{V}_j \oplus \mathbf{O}_j \qquad j \in Z \tag{3.7}$$

with $\mathbf{V}_j \perp \mathbf{O}_j$ and $\oplus$ denotes direct sum. Thus, by iterating the decomposition $J$ times the $V_0$ space can be decomposed as

$$\mathbf{V}_0 = \mathbf{O}_1 \oplus \cdots \oplus \mathbf{O}_{j-1} \oplus \mathbf{O}_j \oplus \mathbf{V}_j \tag{3.8}$$

An arbitrary time series $x(t) \in L^2(\Re)$ can be written as

$$x(t) = \sum_{k \in Z} a_{J,k} \phi_{J,k}(t) + \sum_{j \le J} \sum_{k \in Z} d_{j,k} \psi_{j,k}(t) \quad , \tag{3.9}$$

where the first term represents the approximation on the scale $J$ and the second term represents the details on the scale $J$ and all finer scales. Together the wavelet coefficients $a_{J,k}$ of the approximation and the $d_{j,k}$ of the details form the discrete wavelet transform of the original time series $x(t)$.

In wavelet MRA the wavelet approximation coefficients $a_{J,k}$ and detail coefficients $d_{j,k}$ on adjacent scales are related by the decomposition

$$a_{j,k} = \sum_{n \in Z} h^*_{n-2k} a_{j-1,n} \quad , \quad d_{j,k} = \sum_{n \in Z} g^*_{n-2k} a_{j-1,n} \quad , \tag{3.10}$$

as well as by the reconstruction

$$a_{j-1,k} = \sum (h_{k-2n} a_{j,n} + g_{k-2n} d_{j,n}) \, , \tag{3.11}$$

as shown in Figure 3.10 in a pyramid structure. The coefficients $h_n$ and $g_n$ are given as

$$h_n = \int \phi(t) \phi_{-1,n}(t) dt \quad \text{and} \quad g_n = (-1)^n h^*_{1-n} \tag{3.12}$$

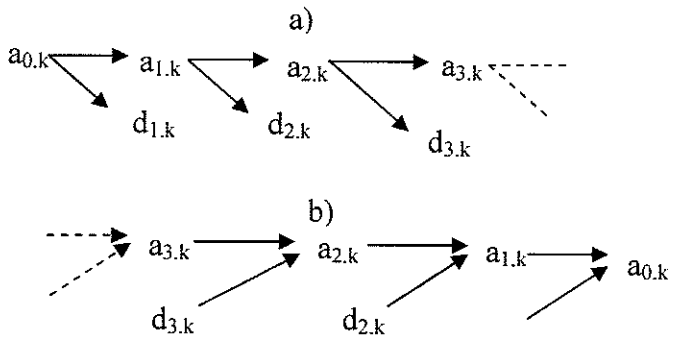


**Figure 3.10.** Pyramid scheme of wavelet a) Decomposition and b) Reconstruction.

In practice, a discrete time series $x_k$ acquired at times $t_k = k\Delta t, \quad k = 1, \cdots, N,$ with constant sampling time $\Delta t$, at its original resolution is assumed the 0-th level approximation sequence; i.e., $a_{0,k} = x_k$ [59]. Therefore, the number of scales $J$ is limited to the largest integer smaller than or equal to $\log_2 N$. Using the subband coding scheme the approximation and detail coefficients are generated using a pair of finite impulse response lowpass and highpass filters, H, G and the signal can be reconstructed using their adjoints $H^*$, $G^*$, respectively, [58] as shown in Figure 3.11 defining a multiresolution decomposition-multiresolution reconstruction (MRD-MRR) scheme.

### III. Wavelet Denoising

The wavelet based denoising assumes that analysis of time series at different resolutions might improve the separation of the true underlying signal from noise. The DWT is linear and orthogonal, thus transforming white noise in the time space to white

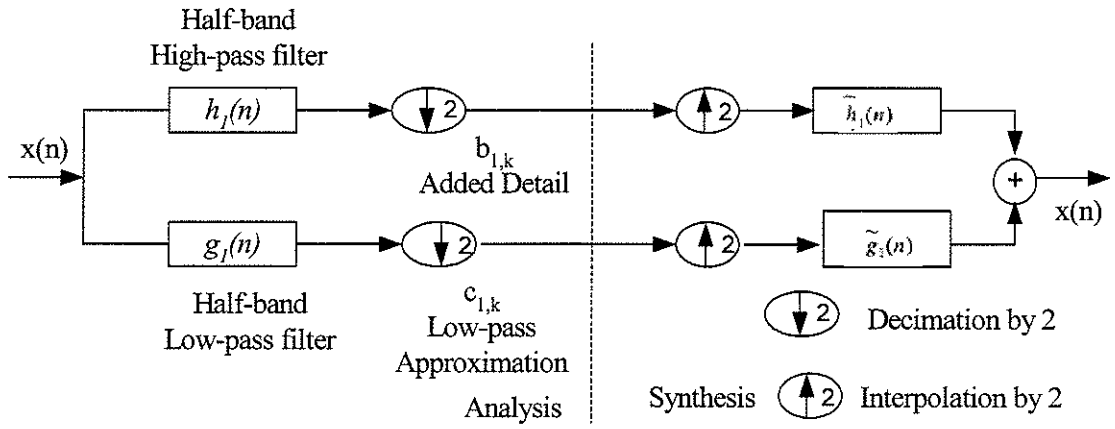


**Figure 3.11.** One-level multiresolution decomposition and reconstruction.

noise in the space of the wavelet coefficients [60]. The detail wavelet coefficients posses high absolute values only in the intervals of rapid time series change. These properties led Donoho and Johnstone to propose denoising with thresholding [60, 61], which consists of the following steps:

- A time series is transformed to the wavelet coefficients $a_{J,k}$ of the approximation and wavelet coefficients $d_{j,k}$, $j = 1, 2,\ldots, J$, of the details.
- The wavelet coefficients $d_{j,k}$ of the details on each scale , $j = 1, 2,\ldots, J$, are separately thresholded with the threshold, $\tau$ as

$$\tilde{d}_{j,k} = \mathrm{T}(d_{j,k}, \tau_j) \quad , \tag{3.13}$$

where $\mathrm{T}(d,\tau) = \begin{cases} 0, & |d| \le \tau \\ d, & otherwise \end{cases}$ or $\mathrm{T}(d,\tau) = \begin{cases} 0, & |d| \le \tau \\ d - sign(d)\tau, & otherwise \end{cases}$

for hard and soft thresholding, respectively.

From the approximation coefficients $a_{J,k}$ and modified detail coefficients $\tilde{d}_{j,k}$, $j = 1, \cdots, J$ the denoised time series is reconstructed. Selecting the threshold is the most critical part of denoising.

### IV. The WT-based Adaptive Filtering Algorithm

The WT-based AF was first proposed *in* [62] to separate discontinuous adventitious sounds from vesicular sounds based on their "nonstationary" characteristics assuming the fact that "nonstationary" part (explosive peaks) of a signal in time domain produces large WT coefficients (WTC) over many wavelet scales whereas for the "stationary" part (noisy background) the coefficients die out quickly with increasing scale. Therefore, it is possible to characterize the WTC with respect to their amplitudes; most significant coefficients at each scale with amplitude above some threshold correspond to nonstationary signal in time domain and the rest corresponds to stationary part of the signal. Consequently, a wavelet domain separation of WTC corresponds to time domain separation of stationary and nonstationary part of a signal. In this way, the nonstationary part of the input signal is separated from the stationary one. The details of the algorithm can be found in [62]. The algorithm was employed for the adaptive thresholding and separation of HS from LS signals [17]. In their study, desired (LS) and unwanted (HS) portions of a signal were separated through iterative Multiresolution Decomposition and Multiresolution Reconstruction (MRD-MRR) based on hard thresholding of the WTC. At iteration $k$ the WTC of an $N$-sample input signal, e.g., a LS recording, $f(\lambda)$, $\lambda = 1,\ldots, N$, truncated if necessary so that $N$ is a power of two, at $m$ adjacent resolution scales ($m = 1,\ldots, M$; $M = log_2(N)$) were calculated using previously

defined orthonormal bases [63]. The resulting WTC at scale $j$ were compared to a threshold defined as

$$THR_j^k = \sigma_j^k \cdot F_{adj}\ , \tag{3.14}$$

where $\sigma_j^k$ is the standard deviation of the WTC at scale $j$ during the $k^{\text{th}}$ iteration and $F_{adj}$ is a constant adjusting multiplying factor chosen experimentally based on individual files to keep the threshold at higher value at different scales. The WTC were divided into two groups - coefficients larger than the threshold signal ($WT^{kC}(\lambda)$) and coefficients smaller than the threshold ($WT^{kR}(\lambda)$). The MRR was performed to reconstruct signals $C_k(\lambda)$ and $R_k(\lambda)$ from $WT^{kC}(\lambda)$ and $WT^{kR}(\lambda)$, respectively, representing coherent and residual part of $f(\lambda)$. For the next iteration $k$, $R_{k-1}(\lambda)$ was assigned to $f(\lambda)$. The iterative procedure stops after a fixed number of iterations or after the following Stopping Criterion (STC) is satisfied,

$$STC = \left| E\{R_{k-1}(\lambda)\} - E\{R_k(\lambda)\} \right| < \varepsilon, \qquad 0 < \varepsilon << 1 \tag{3.15}$$

where $E\{\cdot\}$ denoted the expected value and $R_0(\lambda) = 0$. The suggested value for ε was 0.00001 [17, 62]. This STC implies that the residual signal at the current MRD varies by only a very small value from that of the previous MRD. Hence, these waveforms are correlated and any coherent signal is no longer significantly present. After the last iteration ($L$) the nonstationary part of the signal was obtained by superposing the coherent parts, $C_k(\lambda)$ attained at each iteration,

$$NST(\lambda) = \sum_{k=1}^{L} C_k(\lambda), \tag{3.16}$$

and the residual part, $R_k(\lambda)$ was considered as the stationary part of the signal. In this study of heart sound reduction of lung sound the "coherent" signal represents the unwanted HS and the "residual" signal was the denoised LS.

#### 3.2.2.2 WT-based Adaptive Filtering of Lung sound Signal

**I. PSD Analysis of Lung sound Signal**

The LS data from six subjects (5 subjects in Group I and 1 subject from Group II) described in section 3.1 was used in the study of HS reduction in LS recordings using WT-based AF technique. Artifacts were detected and excluded from the recorded LS signals and the LS segments were sequestered as segments, with and without HS as described in section 3.2.1. The segments within target flow±20% were selected as flow-gated segments where target flows were 7.5 ml/s/kg, 15 ml/s/kg and 1.5 ml/s/kg for low, medium flow and breath-hold, respectively. The HS-free segments of LS were used as the standard to measure the effectiveness of the WT-based AF technique used in this study.

The average PSD of the HS-free segments was calculated using 100 ms data samples and Hanning window with 50% overlap between successive segments. The average PSD was also calculated for the LS segments including HS, to provide reference spectra of the segments including both LS and HS. The postulation of this study was that the PSD of WT-based filtered signal would approach closely the PSD of the reference signal obtained from HS-free segments with very slight distortion of LS as judged by expert listeners. The average power of LS signal, including and excluding HS, were calculated over the following octave frequency bands: 20-40 Hz, 40-70 Hz, 70-150 Hz,

150-300 Hz, and 300-600 Hz and averaged between the subjects. The mean (mean±SE) differences in power for LS signals, with and without HS, were calculated over those frequency bands. The PSD of HS-free breath-hold signals were used as an estimation of background noise.

### II. WT-based filtering of Lung sound Signal

In order to reduce HS, the LS signals were used as an input to the WT-based AF. Since the HS has large peaks in LS recording, HS was considered as nonstationary part of the recorded signal. Thus, the output of WT filter given in (3.16) was the HS noise and the remaining signal $R_L(\lambda)$ was the denoised LS. As in [17], the calculation of WTC was based on orthonormal bases introduced by Daubechies [63], using quadrature mirror filters (QMFs) of eight coefficients and the adjusting parameter, $F_{adj}$ for thresholding the coefficients were varied between 2.5 to 3.0 depending on individual subject and flow rates.

### III. Analysis of the Performance of the WT-based Filtering

The effectiveness of the WT-based AF technique for removing HS from LS recordings was evaluated both quantitatively and qualitatively. The quantitative analysis was done by comparing the average PSD of the original LS and breath-hold signals with the filtered signals with focus on the above mentioned five frequency bands. The mean (mean±SE) power differences between the LS segments with HS and HS-free LS signals, averaged between the subjects, were statistically compared (paired $t$-tests, SPSS® software) to determine the absolute PSD differences between LS with and without HS. Differences with $p < 0.05$ were taken as significant. The outputs of the WT-based

adaptive filter were also subjected to flow- and artifact-gating, and the average PSD of the resulting segments were determined for these signals within the above frequency bands as well. Then, the band-limited PSD values of the filtered signals were compared with those of the original

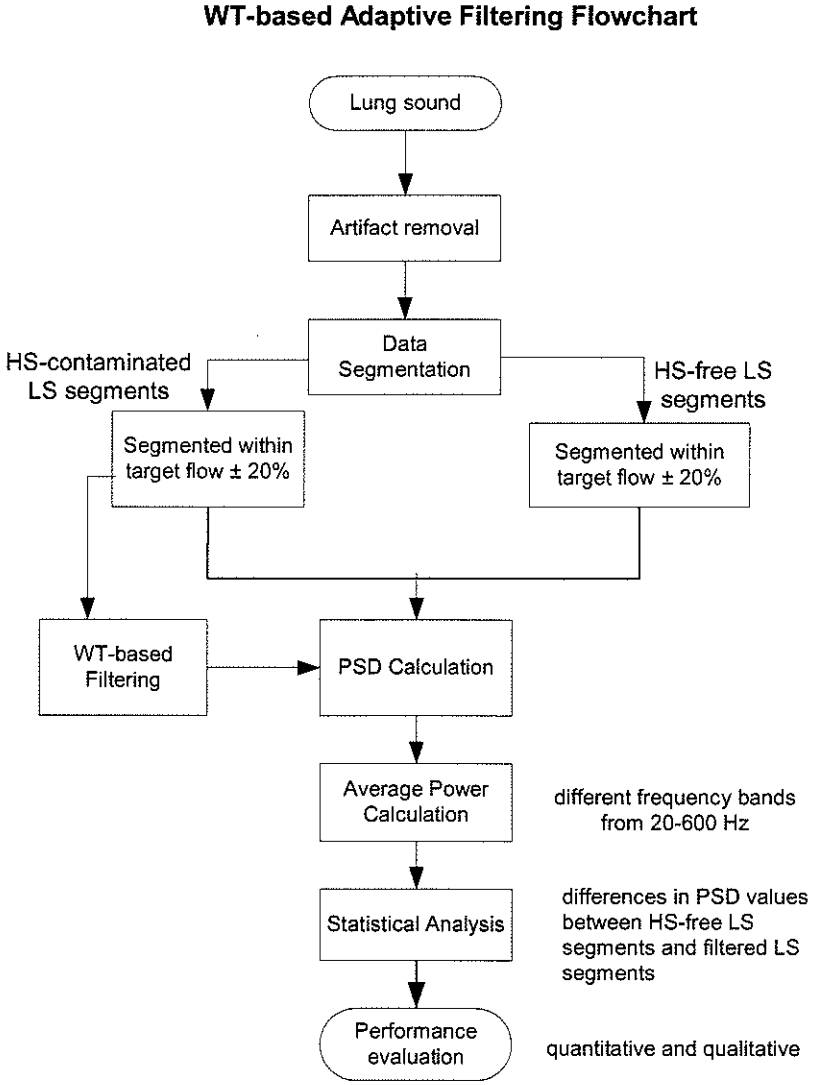


**Figure 3.12.** Flowchart of WT-based adaptive filtering of LS signal.

signals, both including and excluding HS. The hypothesis was that the average PSD values of the filtered signals calculated at five frequency bands would be less than the

PSD values of the original LS segment, and ideally not notably different from those of the HS-free original LS segment.

#### 3.2.2.3 Synopsis of WT-based Adaptive Filtering of Lung sound Signal

Figure 3.12 shows the summary of the WT-based AF of LS signals in the form of flow chart. Data from each subject at each target flow rate was analyzed separately and the mean PSD values at different frequency bands were averaged between the subjects for both original and filtered signals in order to find the effectiveness of WT-based adaptive filter in reduction of HS in LS recordings.

## 3.3 SUMMARY

In this chapter, the details of various digital signal-processing techniques along with a brief overview of the relevant theories and algorithms implemented in this study were described. It also included the instrumentation and data acquisition techniques and particulars of the study subjects from each experimental group. The scheme used to find the LS-flow relationship consisted of artifact removal and data segmentation, calculation of mean flow (*flow*), mean LS amplitude (*mean AMP*) and LS average power ($P_{ave}$), investigation of different frequency bands from which $P_{ave}$ could be computed, examination of several models comprising $P_{ave}$ or *mean AMP* and *flow*, correlation coefficient ($r$) and error calculation between the actual data and estimated data calculated from model coefficients and the data analysis flow chart. An overview of general wavelet denoising technique and the application of WT-based AF technique of HS removal from LS recordings were presented here with a short description of general wavelet theory and the WT-based AF algorithm.

# CHAPTER 4 – RESULTS

## 4.1 RESULTS OF LUNG SOUND-FLOW RELATIONSHIP

The results of investigation of LS-flow relationship for all groups showed a much stronger correlation between flow and $P_{ave}$ than *mean AMP* and flow. Furthermore, the $P_{ave}$-*flow* relationship was best described by the power relationship model (model 3) in both healthy adults and healthy children. The mean±SE value of the power ($\alpha$) was 1.83±0.22 and 2.0±0.17 for healthy adults, 1.79±0.23 and 1.84±0.23 for healthy children for LS signal including and excluding HS, respectively. On the other hand, for asthmatic children the 3$^{rd}$ order polynomial curve (model 4, 3$^{rd}$ degree) demonstrated best fit between $P_{ave}$ and *flow*. The highest correlation coefficients ($r$) between the model variables were observed in the frequency range of 150-450 Hz for healthy subjects and 300-600 Hz in asthmatic children. When comparing the model parameters calculated from different percentage of the flow, it showed best results when the upper 40% to 50% of inspiration was considered. The removal of HS from LS signals showed slight

| Group | Chosen Model | Optimum Freq. band | % of Insp | $r$ (mean±SE) |
|---|---|---|---|---|
| Group I (with HS) | model 3 | 150-450 Hz | 40 | 0.98±0.009 |
| Group I (HS removed) | model 3 | 150-450 Hz | 40 | 0.96±0.01 |
| Group II (with HS) | model 3 | 150-450 Hz | 40 | 0.97±0.03 |
| Group II (HS removed) | model 3 | 150-450 Hz | 40 | 0.95±0.05 |
| Group III (with HS) | model 4 | 300-600 Hz | 50 | 0.98±0.02 |
| Group III (HS removed) | model 4 | 300-600 Hz | 50 | 0.98±0.01 |

**Table 4.1.** Selected models and the corresponding parameters decided for each group.

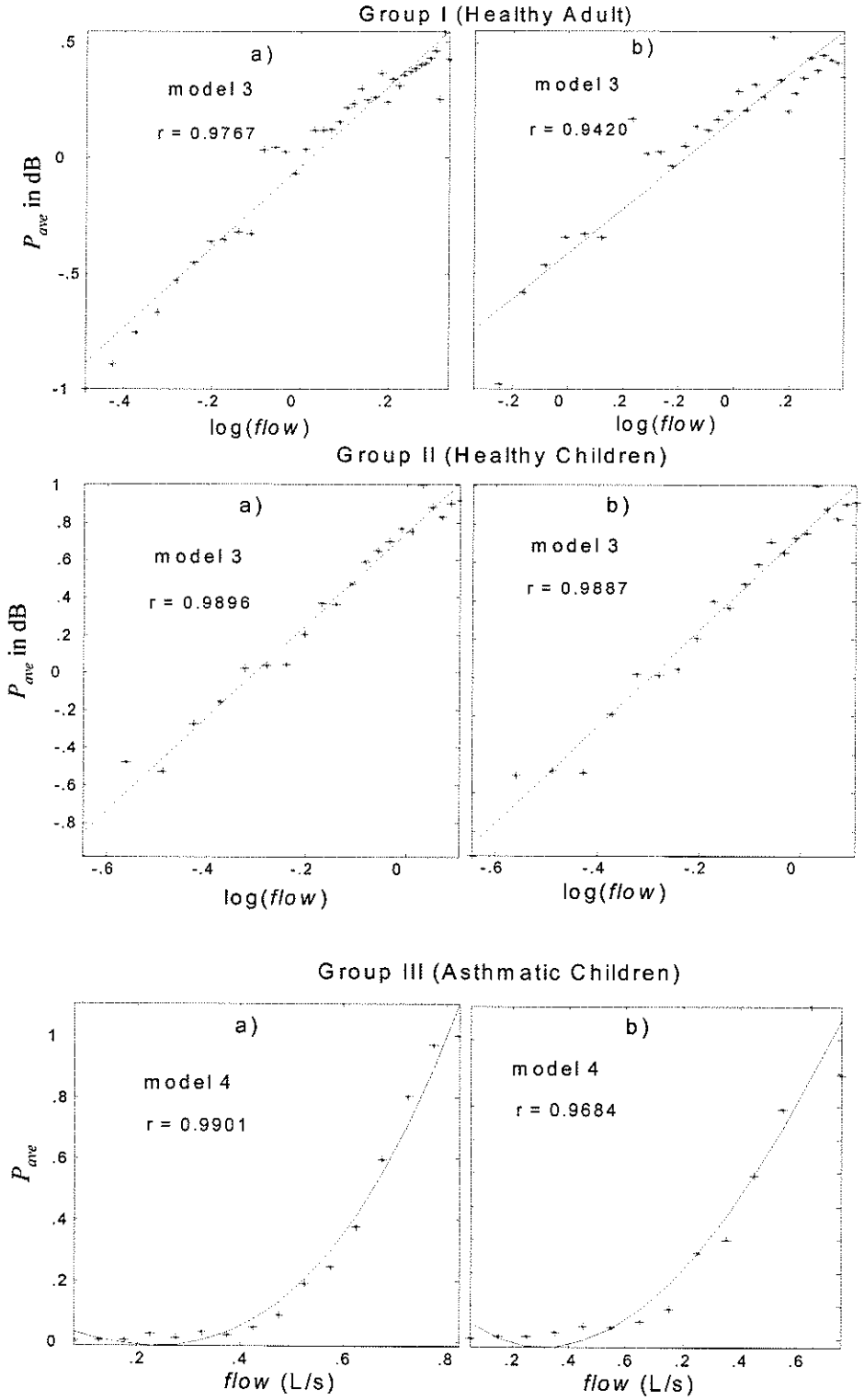


**Figure 4.1.** Examples of curve fitting to the selected models for each group showing $P_{ave}$-*flow* relationship: a) LS signal including HS b) LS signal excluding HS.

differences in the values of model parameters with no change in the model describing the relationship between $P_{ave}$ and *flow* in all groups. The results of optimum model selection with their parameters are summarized in Table 4.1. The results of linear regression analysis and polynomial curve fitting to the selected models for each group are shown in Figure 4.1 for a typical subject in each group. The details of the findings of the study are given in the following sections.

### 4.1.1 LUNG SOUND AMPLITUDE AND FLOW RELATIONSHIP

The results of linear regression analysis of model 1, with $k$ = 1, 2, 3 for healthy adults showed model 1, with $k$ = 1 could best describe the correlation between LS amplitude and flow since it exhibited the highest $r$ with least MSE compared to the model with $k$ = 2, 3. Figure 4.2 shows an example of linear regression analysis to the data of Group I. In case of healthy children, model 1, with $k$ = 2 had the highest $r$ and least MSE for most of the subjects (7 out of 10) and also when averaged between the subjects. Figure 4.3 shows an example of linear regression analysis of model 1 for the data from a healthy child. The models were investigated for the LS signals, both including and excluding HS. It was noted that there was no considerable effect of the HS reduction on the model parameters (Figure 4.2 and Figure 4.3) as well as on the model selection.

However, for asthmatic children the value of $r$ was less than 0.5 for all the values of $k$, which demonstrated that there was a weak relationship (Table 3.2) between model variables. Thus, the LS *mean AMP-flow* model was not a good representative of LS amplitude-flow relationship for asthmatic children. Figure 4.4 illustrates the result for a typical asthmatic subject.

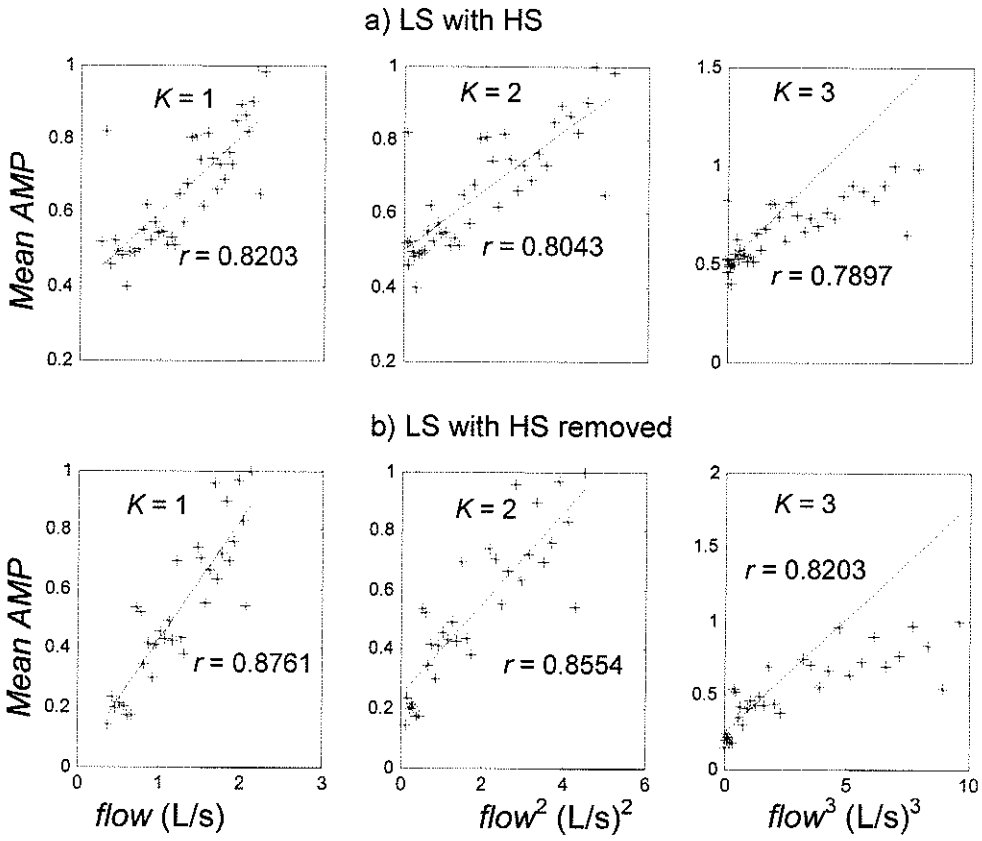


**Figure 4.2.** Linear regression analysis of model 1 ($k = 1, 2, 3$) representing the relation between LS amplitude and flow for a healthy adult: a) LS signal including HS b) LS signal excluding HS.

In *mean AMP* and *flow* modeling study, the models were examined with different percentage of inspiratory flow and the corresponding sound amplitude for all data sets. The results showed small differences in the values of the model parameters. However, the results were most consistent with highest $r$ and least MSE when the upper 40% of flow was taken into account. Therefore, *mean AMP* and *flow* corresponding to upper 40% of target flow were used in model selection study.

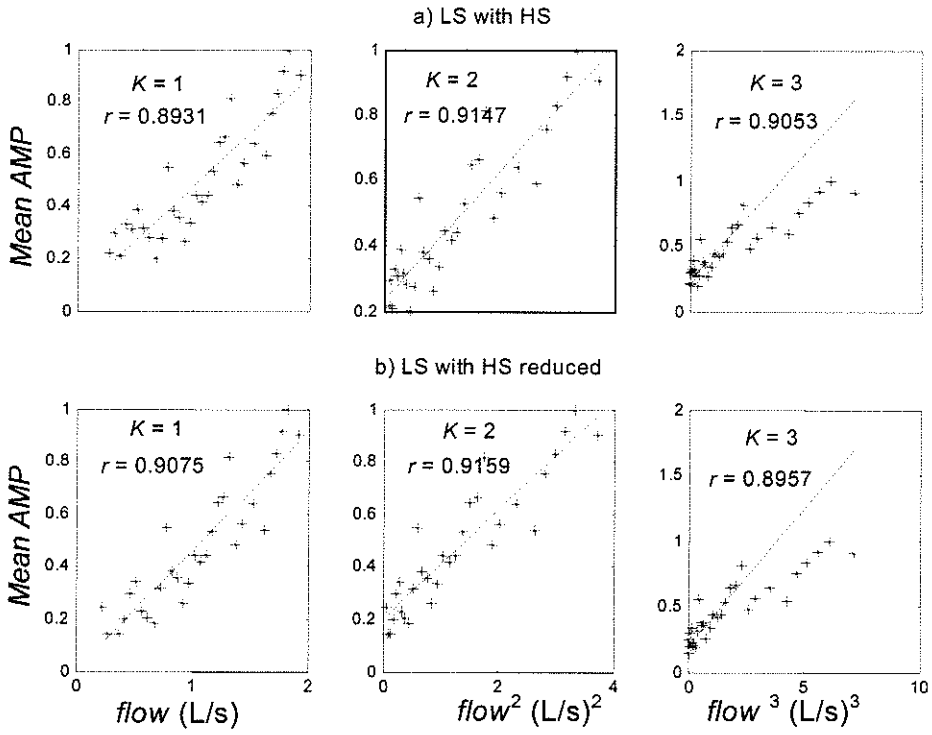


**Figure 4.3.** Linear regression analysis of model 1 ($k = 1, 2, 3$) representing the relation between LS amplitude and flow for a healthy children : a) LS including HS b) LS excluding HS.

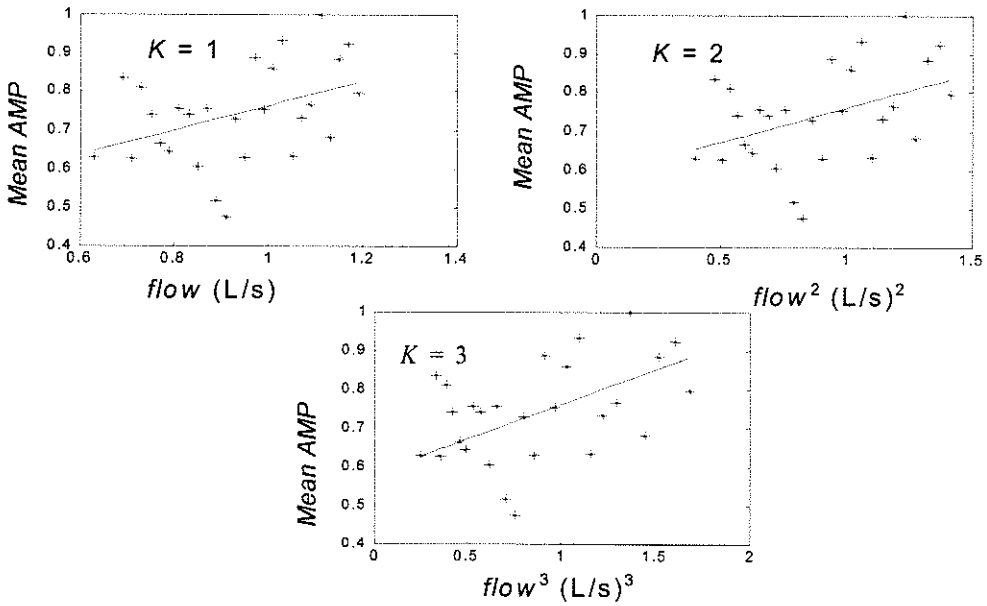


**Figure 4.4.** Linear regression analysis of model 1 ($k = 1, 2, 3$) representing the relation between LS amplitude and flow for an asthmatic subject.

### 4.1.2 LUNG SOUND AVERAGE POWER AND FLOW RELATIONSHIP

Results of linear regression analysis to the models consisting of $P_{ave}$ and mean *flow* (models 2 and 3) and the polynomial curve fitting (model 4) revealed that there was an obvious relationship between LS average power and respiratory flow. The values of $r$ were bigger than 0.8 for all the models which proved a strong positive correlation between $P_{ave}$ and *flow* (Table 3.2). Comparison of different models for healthy adults and healthy children showed the power relationship model (model 3) to be the right most

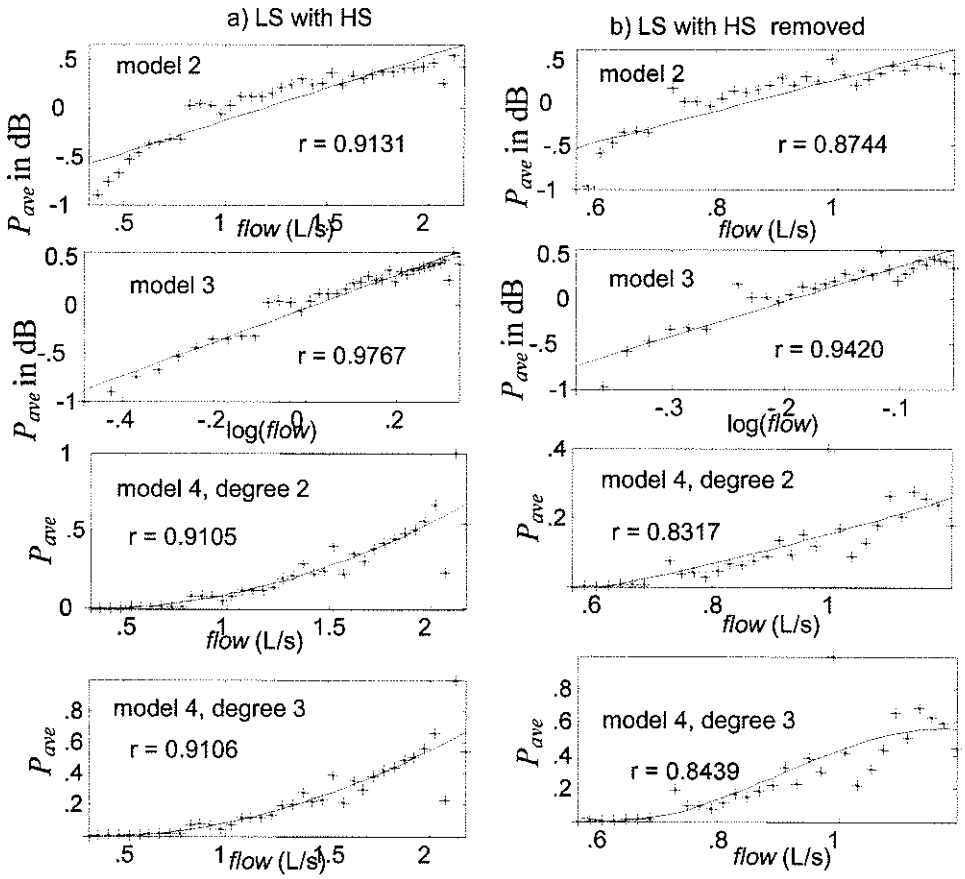


**Figure 4.5.** An example of curve fitting to the models showing $P_{ave}$-*flow* relationship for a healthy adult. $P_{ave}$ was calculated at 150-450 Hz frequency band, data of upper 40% of each inspiration was used for the analysis.

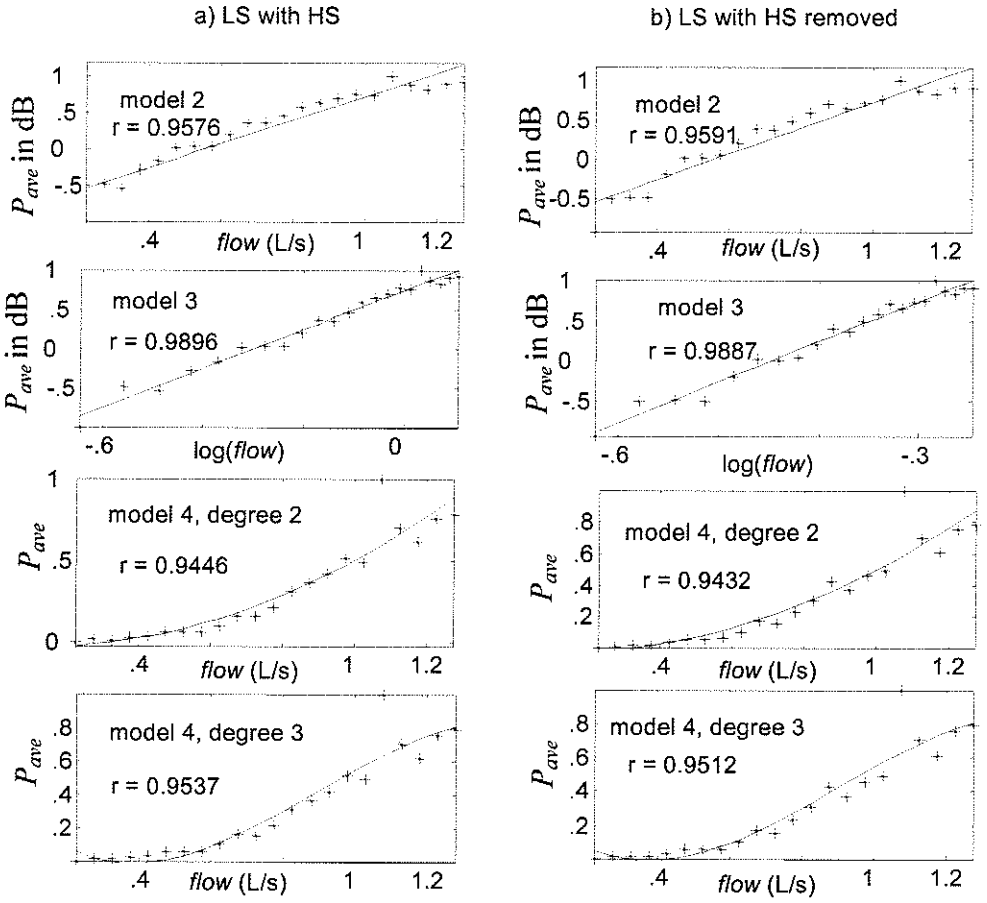


**Figure 4.6.** An example of curve fitting to the models showing $P_{ave}$-*flow* relationship for a healthy child. $P_{ave}$ was calculated at 150-450 Hz frequency band, data of upper 40% of each inspiration was used for the analysis.

model for the LS signals, with and without HS, and flow when the signals were adopted from healthy adults.. Figure 4.5 and Figure 4.6 show the results for a healthy adult and a healthy child, respectively.

When LS data from asthmatic children were analyzed for model selection, the 3rd degree polynomial showed best fit between $P_{ave}$ and *flow*, as it showed least MSE and highest *r* for six subjects out of seven. The results of linear regression analysis and

| Model | Group – I, Healthy adults (with HS) | Group – I, Healthy adults (HS removed) | Group – II, Healthy children (with HS) | Group – II, Healthy children (HS removed) | Group – III, Asthmatic children (with HS) | Group – III, Asthmatic children (HS removed) |
|---|---|---|---|---|---|---|
| **model 1, $k=1$** | 0.75±0.05 | 0.78±0.04 | 0.85±0.10 | 0.83±0.08 | 0.42±0.12 | 0.52±0.09 |
| **model 1, $k=2$** | 0.70±0.06 | 0.76±0.05 | 0.86±0.10 | 0.88±0.09 | 0.42±0.12 | 0.52±0.09 |
| **model 1, $k=3$** | 0.64±0.07 | 0.73±0.06 | 0.85 ±0.10 | 0.84±0.10 | 0.42±0.12 | 0.52±0.09 |
| **model 2** | 0.94±0.02 | 0.91±0.02 | 0.95±0.02 | 0.94±0.02 | 0.97±0.02 | 0.97±0.02 |
| **Model 3** | 0.98±0.009 | 0.96±0.01 | 0.97±0.03 | 0.96±0.05 | 0.96±0.03 | 0.97±0.02 |
| **model 4 degree 2** | 0.93±0.02 | 0.85±0.09 | 0.93±0.05 | 0.93±0.05 | 0.98±0.02 | 0.92±0.01 |
| **model 4 degree 3** | 0.94±0.02 | 0.85±0.08 | 0.93±0.05 | 0.94±0.05 | 0.98±0.02 | 0.98±0.01 |

**Table 4.2.** Mean (mean±SE) correlation coefficient ($r$) for different models in different groups relating LS *mean AMP* and $P_{ave}$ to *flow*. The maximum value of $r$ is marked as gray for each study group.

polynomial curve fitting are shown in Figure 4.7 for a typical subject, where $P_{ave}$ is calculated over 300-600 Hz for upper 50% of flow signal. The mean values (mean±SE) of $r$ between the estimated data using model coefficients and the actual data for each group and each model are shown in Table 4.2. The selected models were highlighted for each group.

From the LS $P_{ave}$-*flow* relationship modeling study it was observed that the relationships as well as the model's parameter were highly dependent on the frequency band used for $P_{ave}$ calculation. The results showed that below 70 Hz, the relationship could not be defined since there was no specific pattern between $P_{ave}$ and *flow* and the values of $r$ were less than 0.5 for each model. The average error (mean±SE) between

actual and estimated data from model coefficients was the least and $r$ was the highest when $P_{ave}$ was calculated over 150-450 Hz frequency band for Group I and Group II. Therefore, 150-450 Hz was chosen as the optimum frequency band for $P_{ave}$ calculation for Groups I and II. On the other hand, in case of asthmatic children, the optimum frequency band was found to be 300-600 Hz. The parameter values of the selected models with $P_{ave}$ calculated at various frequency bands between 20-600 Hz are shown in Table 4.3 for each group. The optimum frequency bands were highlighted for each group of data set.

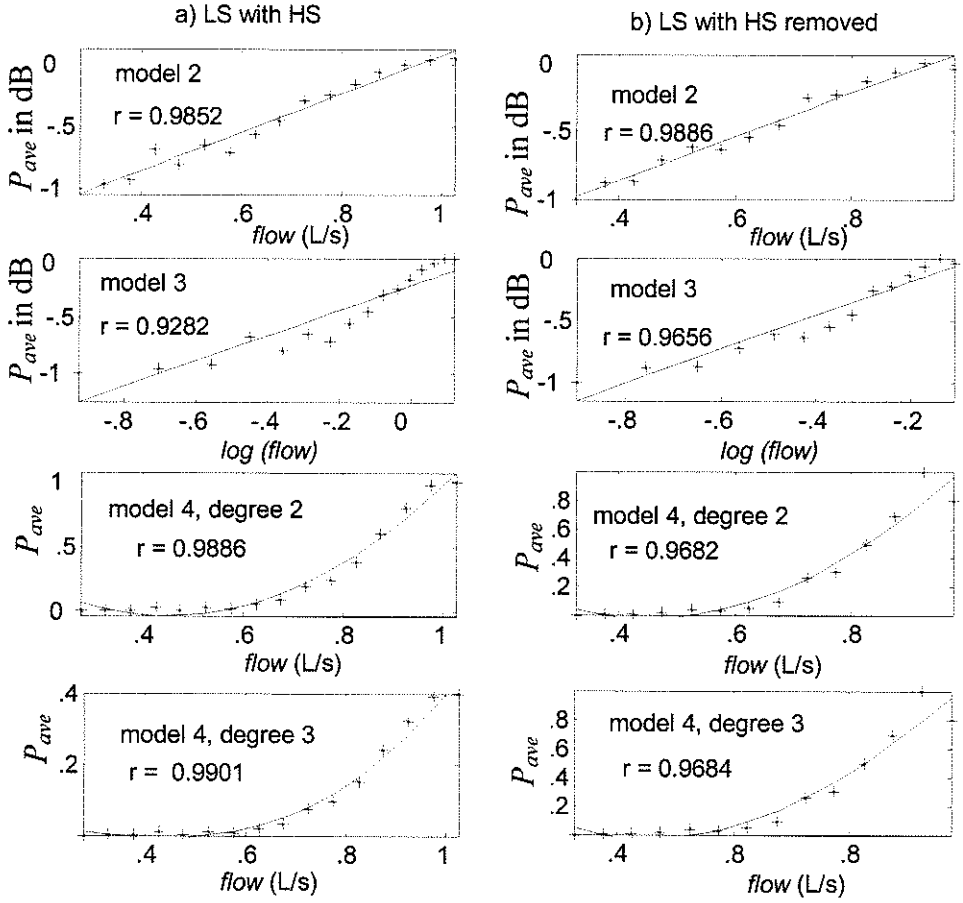

**Figure 4.7.** An example of curve fitting to the models showing $P_{ave}$-*flow* relationship for an asthmatic child. $P_{ave}$ was calculated at 300-600 Hz frequency band, data of upper 50% of each inspiration was used for the analysis.

In order to find the $P_{ave}$-*flow* relationship all the models were tested by taking different percentage of inspiratory flow. Though the results showed small differences in the values of the model parameters, the mean (mean±SE) MSE value was the least and correlation coefficient, $r$, was the highest when upper 40% of flow signal was used for Groups I and II, and upper 50% of flow signal for Group III.

| 20-40 Hz | 40-70 Hz | 70-150 Hz | 70-300 Hz | 70-450 Hz | 100-300 Hz | 100-450 Hz | 100-300 Hz | 150-450 Hz | 300-600 Hz |
|---|---|---|---|---|---|---|---|---|---|
| **Group I, Healthy adults (with HS), model 3, upper 40% of inspiration** | | | | | | | | | |
| 0.50±0.09 | 0.64±0.08 | 0.91±0.07 | 0.92±0.06 | 0.92±0.06 | 0.96±0.02 | 0.96±0.02 | 0.97±0.01 | 0.98±0.009 | 0.93±0.01 |
| **Group I, Healthy adults (HS removed), model 3, upper 40% of inspiration** | | | | | | | | | |
| 0.60 ±0.12 | 0.77±0.11 | 0.93±0.03 | 0.95±0.02 | 0.95±0.02 | 0.95±0.01 | 0.95±0.01 | 0.96±0.01 | 0.96±0.01 | 0.91±0.003 |
| **Group II, Healthy children (with HS), model 3, upper 40% of inspiration** | | | | | | | | | |
| 0.37±0.15 | 0.45±0.25 | 0.83±0.11 | 0.93±0.06 | 0.93±0.54 | 0.95±0.05 | 0.94±0.06 | 0.95±0.05 | 0.97±0.03 | 0.94±0.02 |
| **Group II, Healthy children (HS removed), model 3, upper 40% of inspiration** | | | | | | | | | |
| 0.54±0.18 | 0.71±0.15 | 0.90±0.05 | 0.95±0.03 | 0.96±0.03 | 0.96±0.03 | 0.96±0.03 | 0.96±0.03 | 0.97±0.03 | 0.90±0.03 |
| **Group III, Asthmatic children (with HS), model 4, upper 50% of inspiration** | | | | | | | | | |
| 0.57±0.18 | 0.51±0.25 | 0.71±0.21 | 0.75±0.21 | 0.75±0.21 | 0.91±0.12 | 0.91±0.11 | 0.95±0.02 | 0.96±0.02 | 0.98±0.02 |
| **Group III, Asthmatic children (HS removed), model 4, upper 50% of inspiration** | | | | | | | | | |
| 0.63±0.24 | 0.67±0.14 | 0.81±0.14 | 0.85±0.11 | 0.83±0.14 | 0.96±0.02 | 0.95±0.03 | 0.95±0.04 | 0.96±0.04 | 0.98±0.01 |

**Table 4.3.** Selected model and the corresponding $r$ values (mean±SE) of each group for $P_{ave}$ calculated at different frequency bands between 20-600 Hz. The maximum value of $r$ is marked as gray for each study group.

## 4.2 RESULTS OF WT-BASED ADAPTIVE FILTERING OF LUNG SOUND

### 4.2.1 RESULTS OF PSD ANALYSIS

The PSD analysis of LS signal, including and excluding HS, at low and medium flow rates resulted in significant difference ($p < 0.05$) in the average PSD values up to 150 Hz. This illustrates that most of the HS energy is contained below 150 Hz, where LS has also considerable energy. For breath-hold signals, including and excluding HS, there were significant differences ($p < 0.01$) in average PSD values in all frequency bands at all flow rates. At high flow, however, the difference was considerable below 70 Hz. Hence, the objective of this study was to reduce HS from lung sounds at low and

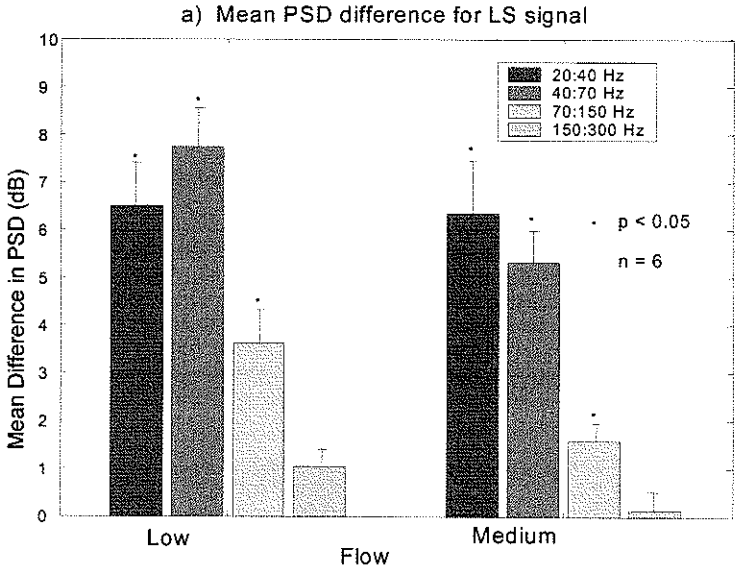

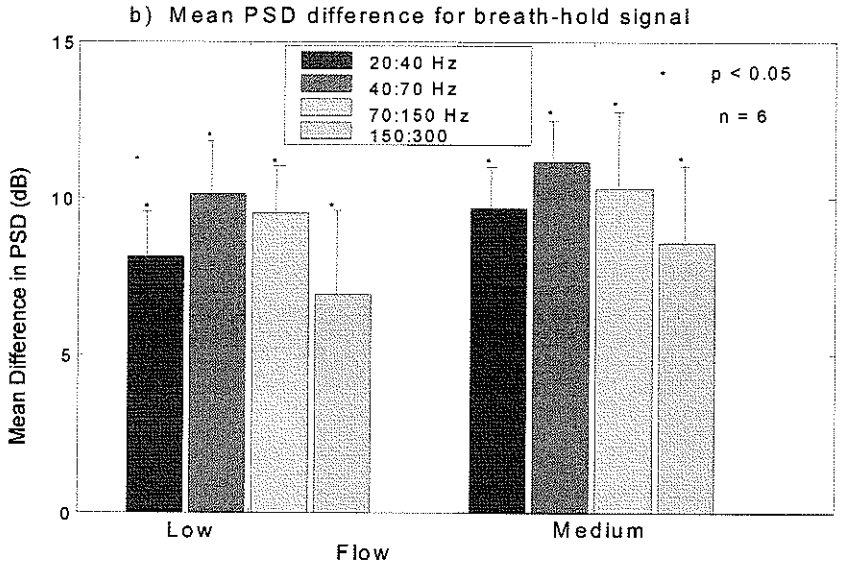


**Figure 4.8.** Differences in average power calculated for LS and breath-hold signals, including and excluding HS, at low and medium flow rates. Error bars represent mean SE, * denotes the significant level ($p<0.05$) medium flow rates.

medium flow rates. Figure 4.8 shows the average PSD differences of original LS and breath-hold signals, including and excluding HS, calculated over the first four frequency bands.

### 4.2.2 WT-BASED ADAPTIVE FILTERING

The wavelet analysis experiments with Daubechies QMFs filters of different lengths (db2 to db12) and with hard and soft thresholding showed that the use of db8

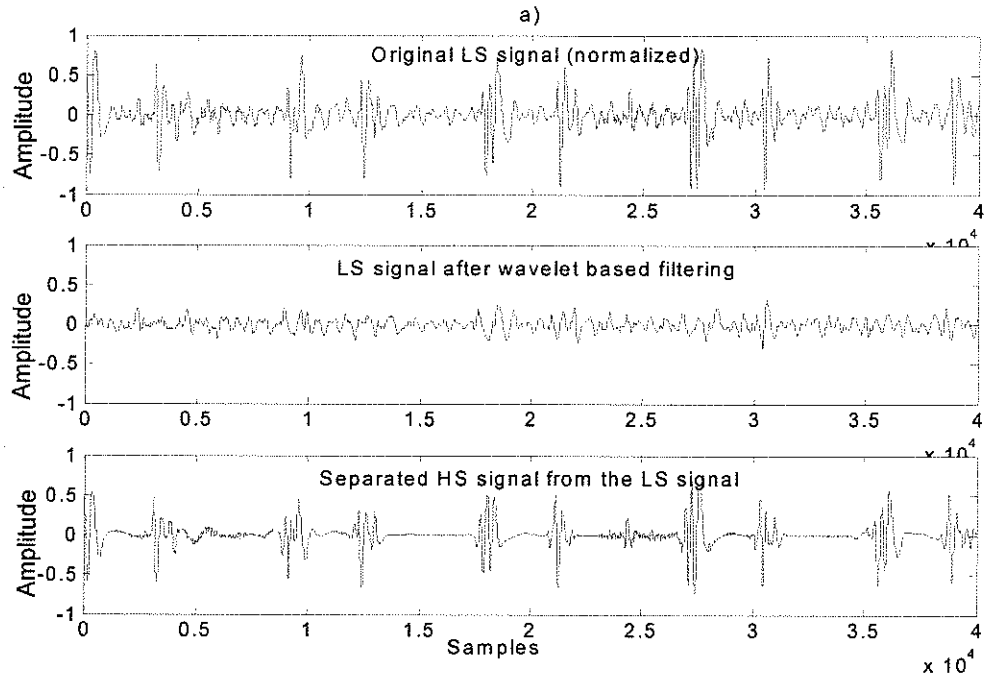


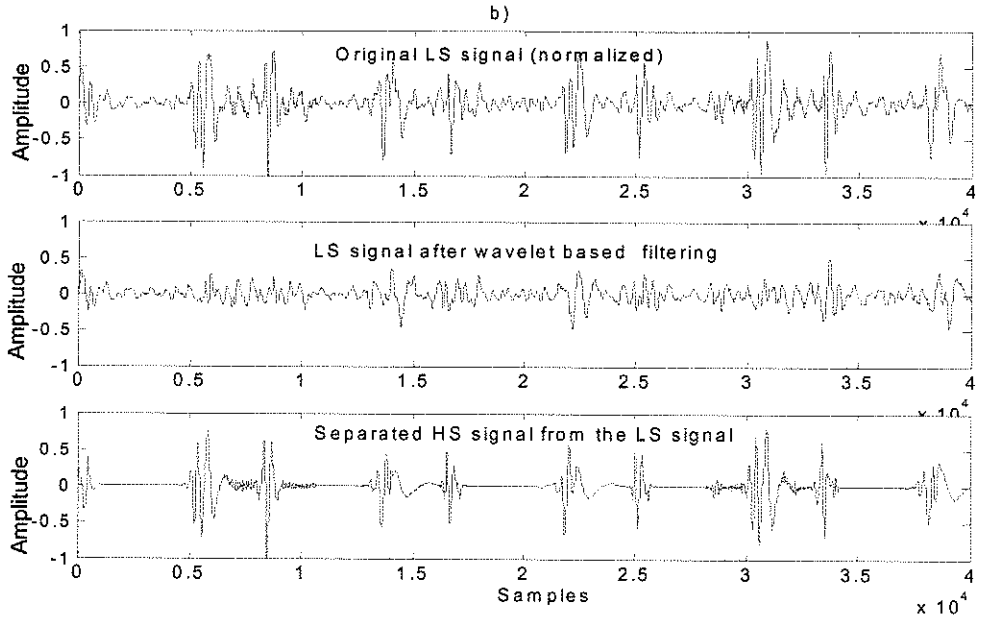

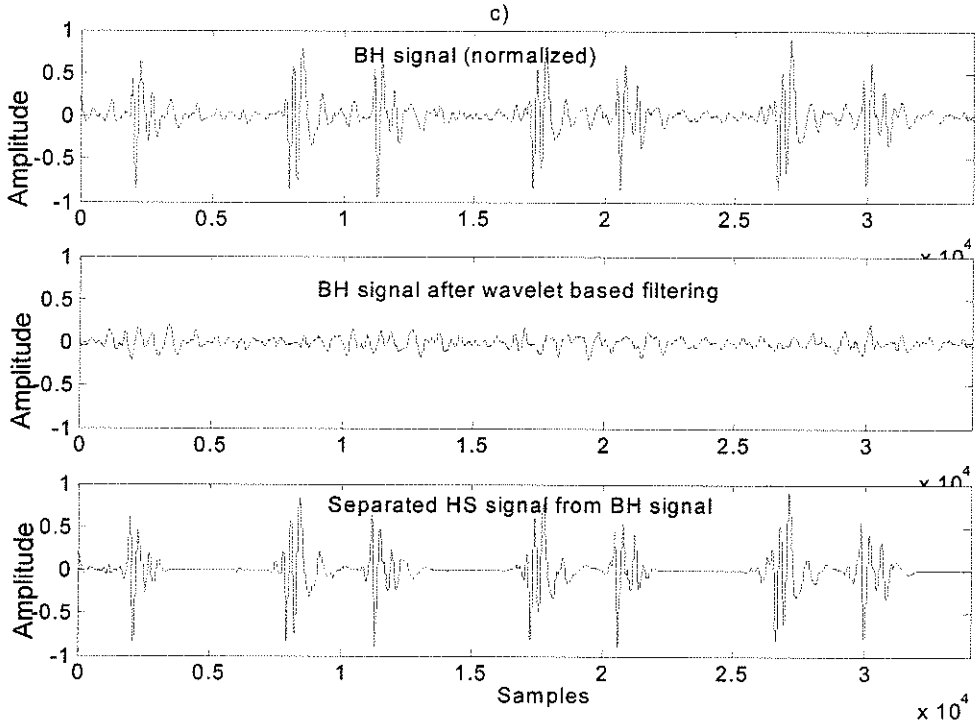


**Figure 4.9.** Separated HS signals using WT-based AF for a typical subject: a) LS signal at low flow rate, b) LS signal at medium flow rate, c) Breath-hold signal.

filter with hard thresholding performed best for separating the stationary and nonstationary part of the LS recordings. It was found that the performance of the WT-based filter was very much dependent on the threshold adjusting parameter, *Fadj*. For low flow rate, it was varied between 2.5 to 2.7 and for the medium flow rate it was adjusted between 2.7 to 3.0. The number of iteration, $L$, needed to converge the algorithm was found to vary between 7 to 10 for $\varepsilon = 0.00001$.

Results of implementation of WT-based AF to the LS and breath-hold signals at low and medium flow rates are shown for typical subject in Figure 4.9. It was seen that the WT- based AF could detect the heart peak locations in LS signal and could separate

those peaks efficiently at any flow rates (Figure 4.9). However, the power spectra of the filtered signals showed pronounced difference when it was compared with the original HS-free segments of LS and breath-hold. The average PSD of the filtered signals along with the average PSD of the original signals, including and excluding HS, are shown in Figure 4.10(a) and 4.10(b) for low and medium flow rates, respectively, and in Figure 4.10(c) for breath-hold signals. The results showed that all flow- and artifact-gated filtered signals had lower average PSD than that of HS-free original signals, specially at frequencies above 100 Hz (Figure 4.10) and the difference was more remarkable for medium flow rate (Figure 4.10(b)). However, the statistical analysis indicated that for the low flow signals the differences of the average PSD values of the filtered LS signals and original HS-free LS signals per frequency band averaged across the subjects were not significant for any frequency band. For the medium flow, the difference was significant for the 70-150 Hz and 150-300 Hz frequency bands (-4.61±1.69 with $p < 0.05$, and –8.22±2.21 with $p < 0.02$, respectively). Moreover, the differences were negative for both low and medium flow rates, except at 20-40 Hz band for medium flow (0.72±2.27), implying that the WT-based AF causes an overall reduction of energy of LS, instead of lessening the power only in areas of HS. Similar analysis applied to the breath-hold signals showed that the differences in average PSD values in breath-hold signals were not significant ($p > 0.13$ ) for any frequency band for the low flow signals and they were significant ($p < 0.02$) only for the 150-300 Hz band for medium flow signals. Table 4.4 shows these differences for filtered LS signals and original HS-free LS signals in low and medium flow rates for both LS and breath-hold signals. The listening inspection of the original and filtered signal showed that WT based filtering could reduce HS to some

extent, while at the same time the original LS signal was attenuated substantially making it a "noise" like signal.

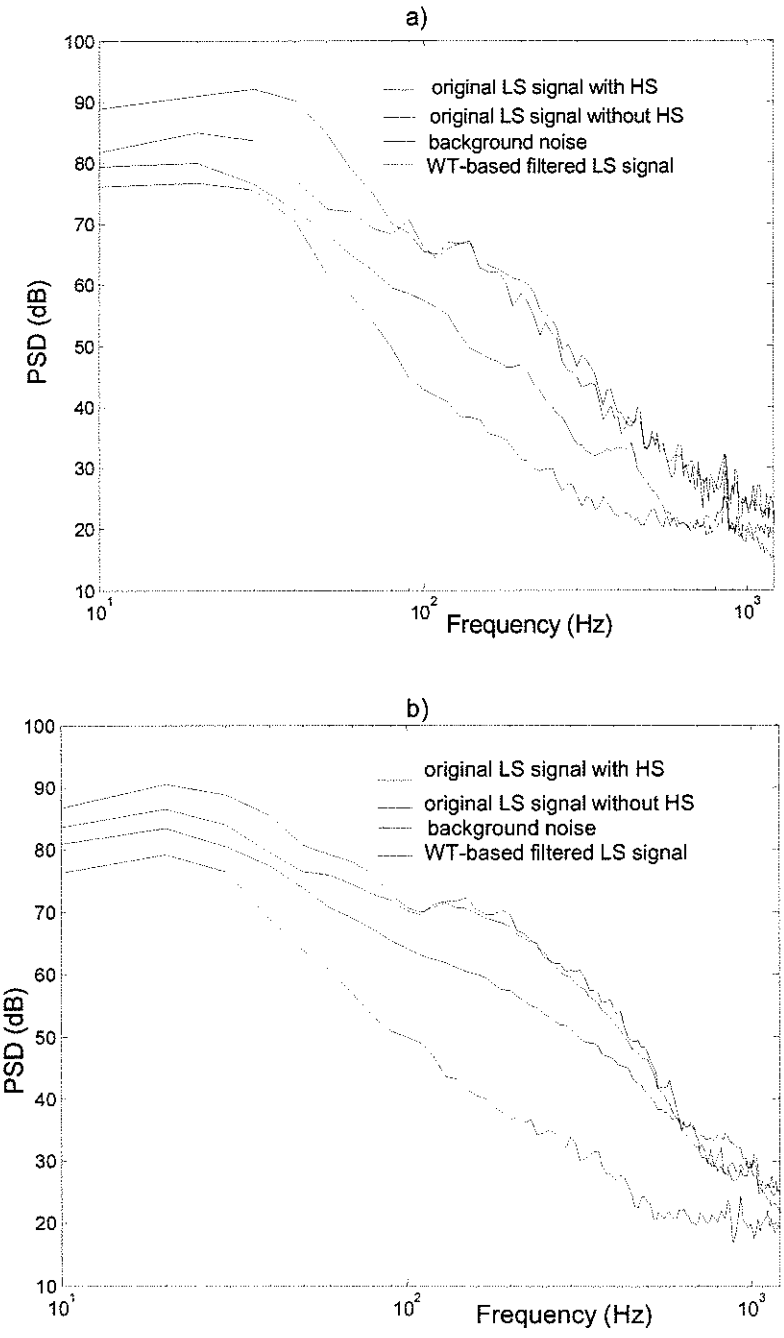

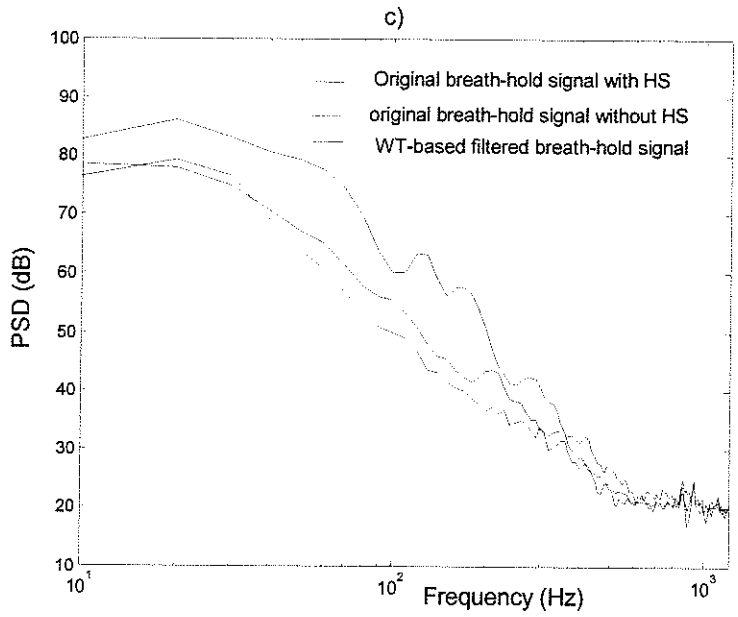


**Figure 4.10.** Power spectra of the original and filtered signals of a typical subject: a) LS signal at low flow rate, b) LS signal at medium flow rate, c) Breath-hold signal.

| Freq / Flow rate | 20-40 Hz | | 40-70 Hz | | 70-150 Hz | | 150-300 Hz | | 300-600 Hz | |
|---|---|---|---|---|---|---|---|---|---|---|
| | Diff 1 | Diff 2 | Diff 1 | Diff 2 | Diff 1 | Diff 2 | Diff 1 | Diff 2 | Diff 1 | Diff 2 |
| **Low** | -1.06 ± 2.51 | 0.62 ± 3.65 | -2.07 ± 2.65 | 0.22 ± 3.82 | -3.83* ± 2.72 | 3.2* ± 3.72 | -5.06 ± 2.39 | 4.71* ± 2.57 | -1.48 ± 1.82 | 5.01 ± 1.79 |
| **Med** | 0.72 ± 2.27 | 2.04 ± 2.25 | -1.0 ± 1.84 | 1.6 ± 2.4 | -4.61 ± 1.68 | 4.17 ± 2.33 | -8.21 ± 2.1 | 4.97 ± 1.23 | -6.01 ± 2.39 | 4.4 ± 1.0 |

**Table 4.4.** Mean power differences (mean±SE) of filtered LS signals and HS-free original LS signals (diff 1), filtered breath-hold signals and HS-free breath-hold signals (diff 2), per flow and frequency bands (* indicates $p < 0.05$).

## 4.3 SUMMARY

The results of LS–flow relationship modeling and WT-based AF of LS signal can be summarized as the followings.

- The LS average power showed higher correlation with respiratory flow than the LS amplitude.
- The relationship between LS average power and flow was found to be different in healthy and asthmatic subjects.
- The best models selected on the basis of the highest correlation coefficient and the lowest MSE were:
    - Healthy adults and children: power relationship model (model 3)
    - Asthmatic children: 3rd order polynomial (model 4, 3rd degree)
- The selection of different percentages of flow did not change the model describing the relationship between flow and LS signal. However, it showed best fit when upper 40% of flow was considered for healthy subjects (both adults and children) and upper 50% for asthmatic children.
- The relationship between $P_{ave}$ and *flow* was dependent on the frequency band at which the LS power was calculated. The most appropriate frequency band was found to be 150-450 Hz for healthy adults and healthy children and 300-500 Hz for asthmatic children to calculate $P_{ave}$.
- The presence of HS in LS recordings did not show any significant effect on the relationship between LS and flow in all the three groups.
- The LS spectral energy was found to be reduced greatly with the WT-based AF and hence resulted in pronounced change in the original signal of interest.

# CHAPTER 5 – ANALYSIS AND INTERPRETATION OF RESULTS

## 5.1 LUNG SOUND–FLOW RELATIONSHIP

The present study was designed to determine the model which could best characterize the LS amplitude and/or average power in relation to flow in both healthy and asthmatic individuals. LS signals recorded from RUL were grouped as three different categories consisted of healthy adults, healthy children and asthmatic children. A wide range of flow, from 0.4 to 3.0 L/s, was used to provide the resolution needed to investigate the LS-flow relationship in both healthy individuals and patients. Four different models defining the LS amplitude-flow and LS average power-flow relationship were investigated. The average LS amplitude was calculated from the envelope of LS signal obtained from the Hilbert Transform of original signal. The LS average power ($P_{ave}$) was calculated from the magnitude of power spectrum of original signal minus the magnitude of power spectrum of the corresponding breath-hold signal. The models were tested for the average power calculated at ten different frequency bands over 20–600 Hz. The overall results showed that $P_{ave}$ was a better parameter than the *mean AMP* to characterize the LS signal with flow. While the exact relationship to describe LS-flow characteristics has yet to be determined with a larger data set, our findings pointed toward power relationship between lung sound average power and flow, $P_{ave} = k\,flow^{\alpha}$, in healthy individuals as it was reported previously by Gavriely and Cugell [28]. Moreover, the relationship was found to change with airway narrowing in asthma. The power relationship model in healthy subjects was found to be independent of the age group and

the values of $r$ computed between the original data and regression lines fitted the power model were much higher (>0.9) than those were found for the models comprising *mean AMP* and *flow* describing stronger linear relationship between log($P_{ave}$) and log(*flow*). It was expected that the removal of HS from LS would not considerably effect the relationship since the frequency band selected to calculate $P_{ave}$ was above 150 Hz whereas the HS have a large effect on LS below 150 Hz. The results showed indeed, HS did not have any effect on the type of relationship, though the model parameters were changed slightly in the presence of HS. The value of $\alpha$ was found to be 1.89±0.57 (mean±SD) and 1.80±0.57 for LS signal with and without HS, respectively, when averaged over all the subjects from Group I and Group II. The value of $\alpha$ found in this study is comparable with that reported by Gavriely et al. [28], which was 1.66±0.35. The small difference might be due to the use of different frequency band in $P_{ave}$ calculation. Gavriely et al. used 100-1000 Hz frequency band in comparison to the 150-450 Hz used in this study. The difference might also be due to the small size of data in both studies and considering the vast variability between the respiratory sounds of the individuals.

A possible explanation of this power relationship between $P_{ave}$ and *flow* could be derived from the theory of turbulent flow in a tube or duct. Flow turbulence is the presumed mechanism for LS generation [27]. The power of the generated sound and turbulent flow in a tube or duct is proportional to the pressure drop associated with flow fluctuations within the tube [64]. When the Darcy friction factor is used, the pressure drop is proportional to the square of flow velocity ($U^2$) divided by the fourth root of the Reynolds number ($Re = \rho.U.d/h$) i.e., $\Delta P \propto U^2/Re^{0.25}$. Thus, assuming constant geometry,

the pressure drop and the generated sound are expected to be proportional to the flow to the power of 1.75. The exponent of flow in $P_{ave}$-*flow* power relationship found in this study (1.89 and 1.8 for LS with and void of HS, respectively) is reasonably close to 1.75 in the above equation.

Lung sounds originate from intrathoracic large and medium size airways and they contain information about their origin and the way they have been transmitted through the lung. Asthma is an inflammatory condition of the bronchial airways. This inflammation causes reversible airway obstruction and bronchial hyperresponsiveness resulting from narrowed airways [31]. Early studies have shown that normal lung sounds change during airway narrowing with a shift of sound intensity toward higher frequencies [65-66] due to a reduction of power at low frequencies [67]. Since most of the LS energy is focused at low frequencies, a reduction in low frequency power causes a decrease in breath sound intensity detectable by auscultation. Hence, it was expected that the pattern of flow-sound relationship changes with asthma. In asthmatic data studied in this thesis, instead of the power relationship between $P_{ave}$ and *flow*, polynomial curve fitting to the $P_{ave}$ vs. *flow* showed better fit to the data in all subjects. This suggested a different mechanism of sound generation in airway narrowing during asthma. Thus, the changes in LS-flow model may be used as a means of detecting the airway narrowing in diseases.

The examination of frequency dependency of the $P_{ave}$–*flow* model showed an increase in LS average power with an increase of flow in all frequencies above 70 Hz in all subjects though the values of the model parameters varied slightly with the frequency range. However, there was no conclusive pattern of $P_{ave}$-*flow* graph for $P_{ave}$ calculated in

the frequency ranges below 70 Hz in all subjects in all study groups (Figure 5.1). Such characteristic of LS average power at low frequencies was expected. It has been found that sound transmission at lower frequencies (below 300 Hz) is mainly due to parenchyma wave propagation [68] and lung parenchyma has been reported to attenuate frequencies below 100 Hz [26]. Moreover, below 100 Hz LS is masked by some extraneous noise such as muscle and cardiovascular sounds. Hence, it was anticipated that at very low frequency bands $P_{ave}$-*flow* relationship could not be defined.

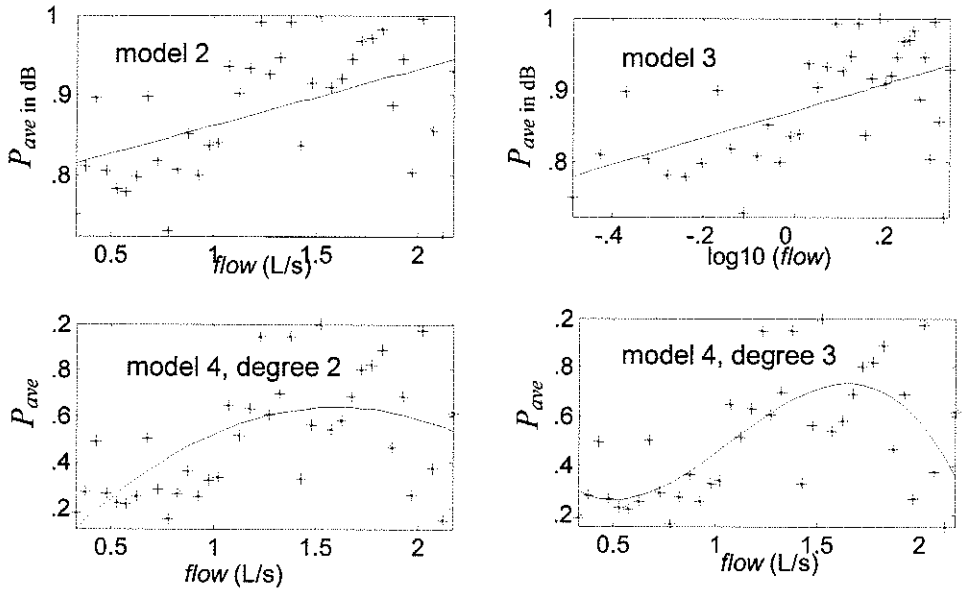


**Figure 5.1.** Effect of frequency band in calculating $P_{ave}$. $P_{ave}$ was calculated at 20-40 Hz frequency band.

The investigation of commonly suggested models that characterize the LS amplitude and flow illustrated a linear relationship between *mean AMP* and *flow* (model 1, $k = 1$) in healthy adults. The values of $r$ (mean±SE) were found to be 0.75±0.04 and 0.78±0.04 for LS signal with and without HS, respectively, which exhibited a moderate linear relationship (Table 3.2) between LS intensity and flow. This result was comparable

to the findings of Kraman [40] who reported that both mean and peak amplitude of LS were linearly related to peak flow when measured in four healthy adults. The reported values of correlation coefficients in that study were 0.77, 0.85, 0.69, 0.89 between *mean AMP* and *flow*, and 0.8, 0.83, 0.79, 0.88 between peak *AMP* and *flow*, in 4 subjects, respectively [40].

In healthy children, however, the results showed that the square of flow (model 1, $k = 2$) was more linearly related to LS amplitude than the first and third power of flow. This result was similar to those described by Shykoff and her co-workers [41], though they reported the results for normal adults. According to Shykoff et al., since LS amplitude is a measure of energy, the relationship may be postulated to be kinetic energy where LS is a function of the square of flow (velocity). The correlation coefficients averaged between ten subjects were found to be 0.86±0.03 (mean±SE) and 0.81±0.02, respectively, for LS signal including and excluding HS.

The reason for the above differences between the type of model in adults and children might be understood in the light of recognizing that body size affects respiratory sounds. The distinct quality respiratory sound in children compared to that in adults is generally due to the sound transmission through smaller lungs and thinner chest walls in children [12, 27]. Pasterkamp et al., [12] found higher median frequency in infants, whereas similar attenuation in power at higher frequencies was found in all ages. It was suggested that the different resonance behavior of a small thorax or less contribution of low frequency muscle noise may explain the difference of normal LS in infants compared with older children and adults [12]. Consequently, the LS amplitude and flow were

speculated to show different relationships in children and adults as it was the case in this study. However, it was noted that the differences in correlation coefficient values were not significant between the first two models (Table 4.2). Hence, investigation with a larger data set may give slightly different results for both groups. The number of subjects that participated in Shykoff et al. [41] and Kraman's [40] studies were 8 and 4, respectively, in comparison to the data adopted from 10 healthy children and 5 healthy adults in this study.

It is anticipated that at very low flow LS may not be detected. Hence, flow must exceed some threshold value to produce the measurable acoustic properties of the thorax. Practically, below approximately 0.3 L/s, the sound amplitude did not exceed the background noise found by previous researchers [10]. Therefore, one of the objectives of this study was to investigate different percentage of target flow to select the best flow region for deriving the LS-flow relationship. In this research, the upper 40% and 50% of target flow gave the most consistent and reliable results in healthy subjects and patients, respectively. In similar studies, Kraman calculated *mean AMP* of each 25 ms segment when the flow exceeded 1.4 L/s for each inspiration [40] and Gavriely et al., [20] acquired data for six different target flows where the flow signal existed within target flow±15%.

Recent respiratory acoustical analyses indicate potential use for clinical application. A series of recent experiments, using bronchial challenge, showed that even in the absence of wheezes, significant changes in the intensity and frequency spectra of breath sounds occur with fairly small changes in the forced expiratory volume in one

second, thus indicating the degree of airflow obstruction [66-67]. Gavriely et al. [69] showed that changes in LS spectra may be used as a means of detecting the early stages of airway diseases though the LS used in his study included wheezes. The future holds the prospect of using acoustic mapping of the surface of the chest wall to non-invasively measure regional ventilation and airflow obstruction within the lungs [7].

The results of this study have shown high correlation of flow signal with spectral power of the LS signal. The $P_{ave}$-*flow* relationship model may be used to estimate respiratory flow by acoustical means which will considerably simplify instrumentation in diagnosis of swallowing dysfunction, sleeping disorder control, monitoring the breath of unconscious patients and so on. The findings have also shown promise to detect abnormalities such as detecting airway narrowing in asthma as the pattern of $P_{ave}$-*flow* relationship changes with abnormalities. Overall, these new findings pave the way for investigating the acoustical properties of respiratory system to improve their use for diagnostic purposes.

## 5.2 WT-BASED ADAPTIVE FILTERING OF LS SIGNAL

The lower spectral limit of normal LS is usually considered above 100 Hz due to the interference of non-respiratory sounds such as heart sounds. Several techniques of reducing interference of HS from LS have been proposed over the last few years. However, the problem has still remained as a challenge because each method has its own disadvantages. One way to tackle the HS interference with LS is to use a method that simply disregards the parts of the LS that include HS by the use of simultaneous record of ECG signal called "ECG-gating", where only the LS segments within the last 30% of the

R-R interval, which are free of HS, are analyzed [45]. This method provided a base for spectrum analysis of the LS absolutely free of HS. However, in doing so most of the recorded sound segments remain unutilized and segmenting the short-duration sections may introduce artifacts while listening to the signal. In addition, it needs an extra recording of ECG signal. Thus, an alternative method of reducing HS in LS has to be investigated so that the spectra of signals from alternative method would follow the spectra of the HS-free LS signals. In this study, the effectiveness of one of the proposed methods using wavelet analysis has been investigated in comparison to the manually obtained HS-free LS signals.

WT-based filter proposed by [17] was implemented to the LS signals recorded at low and medium flow rates. Since most of the HS energy resides below 150 Hz, it was expected that after processing the reduction of energy would be only in the low frequency region and the remaining spectrum would remain unaffected. It was evident from the time domain signals that the amplitude of LS signals decreased slightly after the WT-based filtering (Figure 4.9). The quantitative analysis of HS-free LS signals and filtered LS signals supported this observation. The PSD of filtered LS signals and the PSD of HS-free LS signals were significantly different for both low and medium flow rates in the 70-150 and 150-300 Hz and in addition, the differences were negative (Table 4.4). This shows that the LS signals have experienced an overall reduction in energy by the WT-based filtering (Figure 4.10(a) and (b)) and thus, the signals that are of interest have been altered. The same effect was found for the breath-hold signals in the frequencies above 70 Hz (Figure 4.10(c)) though the differences in PSD values were positive (Table 4.4) in this case. Consequently, the PSD of filtered breath-hold signals were higher than the PSD

of HS-free breath-hold signals. The qualitative analysis also revealed similar results that the LS signals were distorted with some additive noise by WT-based adaptive filtering.

In classical time series denoising approaches, the noise is assumed to be Gaussian white noise. The denoising technique in wavelet transform domain assumes that wavelet transform localizes the signal energy in a limited number of wavelet coefficients. On the other hand, the orthogonal transform of stationary white noise results in stationary white noise [60-61]. Thus, the expected noise energy is spread over all coefficients. If this energy is not very large, noise has a relatively small influence on the important large signal coefficients. Hence, thresholding of the amplitude of the coefficients is possible, which eliminates wavelet coefficients smaller than the threshold, and keeps the larger ones for further estimation of noiseless coefficients. In our case of separating HS from LS, LS was considered as noise. However, it could be noticed that the PSD of LS follows colored noise pattern rather than the white noise with dominant components at frequencies below 300 Hz. Moreover, the HS energy overlaps with lung sound in the frequencies below 150 Hz. Consequently, separating the wavelet coefficients corresponding to HS may also contain information about LS. Furthermore, reconstruction of LS signal with these coefficients degrades the quality of original signal.

# CHAPTER 6 – DIRECTIONS FOR FUTURE RESEARCH

Lung sounds have been used as indicators of respiratory health and disease since antiquity. The diagnosis of diseases is facilitated by pulmonary auscultation using stethoscope since its invention by Laënnec in 1817. In recent years, the inventions of more sensitive methods, specific to respiratory assessment, have aided to collect more information of clinical utility from respiratory sounds. Researchers have been exploring to take advantage of modern technology and computerized sound analysis to effectively aid the day-to-day diagnosis of respiratory patients. One of their notable successes is computerized digital respiratory sound analysis in ambulatory care [27]. Researchers are also making strides to combine processing power, storage, miniaturization of components and analysis programs into small hand-held computerized stethoscopes which will further aid the clinicians with additional information than traditional stethoscopes.

In clinical application, the computerized analysis of LS is expected to be more supportive when it is based on mathematical models of the underlying physical mechanisms of respiratory sound production., such models will facilitate the understanding of the interaction of mechanical forces, flow and sound transmission within the respiratory tract and can also relate to different physiological conditions. Hence, this study was aspired to find a mathematical model that describes the relationship between respiratory flow and the corresponding lung sound. The results proposed power relationship between LS average power and flow in normal study subjects and higher

order nonlinear relationship in asthmatic children. However, experiments with a larger number of subjects are required to confirm the results.

LS-flow relationship varies at different locations of the chest surface [27]. Previous studies found that the low frequency sound amplitude in the right anterior upper lung was significantly greater than that measured at corresponding locations in the left lung [24, 27]. Gavriely et al. [28] observed statistically significant differences in sound amplitude at equal flows between the left and right lung. Therefore, studies of LS-flow relationship at different locations on chest surface may reveal the differences in flow turbulence and sound generation for regional pulmonary ventilation. Future work may include the investigation of models with LS recorded at different locations on the chest surface.

The breath sound intensity recorded at the chest wall during inspiration and expiration is very different and normally, inspiratory sounds are found to be louder than the expiratory sound [30]. Gavriely and co-workers [28] found the amplitudes of inspiratory anterior lung sound are twice of that of the expiratory sound, and the inspiratory posterior lung sounds amplitudes are 140% stronger than those during expiration. Moreover, the frequency spectra of inspiration and expiration are different [12, 20]. Therefore, the models should be investigated separately for inspiratory and expiratory phases.

The HS-free segments of LS signals were obtained by audio-visual means. The drawback of this method is - many of the LS segments get rejected and splicing the

segments would introduce artifacts. Moreover, manual rejection of HS segments might not give the best results due to human error. Recently proposed RLS technique has shown promise in localizing and reducing HS in LS recordings [53]. In future, this technique could be used to get HS-free segments of LS to get more accurate results.

Overall, the findings of the current study are promising in extracting changes in LS-flow relationship between asthmatic patients and healthy individuals. This result, once validated with a larger number of subjects, may be used as an indicator of airway narrowing in asthma.

# BIBLIOGRAPHY

[1] H. Pasterkamp, J. Schafer and G. R. Wodicka, "Posture-dependent change of tracheal sounds at standardized flows in patients with obstructive sleep apnea," *Chest*, vol. 110, pp. 1493–1498, 1996.

[2] A. B. Bohadana, N. Massin, D. Teculescu and R. Peslin, "Tracheal wheezes during methacholine airway challenge (MAC) in workers exposed to occupational hazards," *Respir. Med.*, vol. 88, pp. 581–587, 1994.

[3] A. Avital, E. Bar-Yishay, C. Springer and S. Godfrey, "Bronchial provocation tests in young children using tracheal auscultation," *J. Pediatrics*, vol. 112, pp. 591–594, 1988.

[4] S. Rietveld and L. H. Rijssenbeek-Nouwens, "Diagnostics of spontaneous cough in childhood asthma: Results of continuous tracheal sound recording in the homes of children," *Chest*, vol. 113, pp. 50–54, 1998.

[5] M. Yonemaru, K. Kikuchi, M. Mori, A. Kawai, T. Abe, T. Kawashiro, T. Ishihara and T. Yokoyama, "Detection of tracheal stenosis by frequency analysis of tracheal sounds," *J. Appl. Physiol.*, vol. 75, pp. 605–12, 1993.

[6] A. Sanna, P. Lorimier, B. Dachy, A. D'Hondt and R. Sergysels, "Value of monitoring of tracheal respiratory sounds in the diagnosis of nocturnal respiratory dysrhythmias," *Acta. Clinica. Belgica.*, vol. 46, pp. 159–64, 1991.

[7] J. E. Earis and B. M. G. Cheetham, "Future perspective of respiratory sound research," *Eur. Respir. Rev.*, vol. 10(77), pp. 641-646, 2000.

[8] S. S. Kraman, H. Pasterkamp, M. Kompis, M. Takase and G. R. Wodicka, "Effects of breathing pathways on tracheal sound spectral features," *Respir. Physiol.*, vol. 111, pp. 295–300, 1998.

[9] Y. Ploysongsang, J. A. Pare and P. T. Macklem, "Correlation of regional breath sound with regional ventilation in emphysema," *Am. Rev. Respir. Dis.,* vol. 126, pp. 526–529, 1982.

[10] G. Soufflet, G. Charbonneau, M. Polit, P. Attal, A. Denjean, P. Escourrou and C. Gaultier., "Interaction between tracheal sound and flow rate: a comparison of some different flow evaluations from lung sounds," *IEEE Trans. Biomed. Eng.*, vol. 37, pp. 384–391, 1990.

[11] G. Charbonneau, M. Sudraud and G. Soufflet, "Method for the evaluation of flow rate from pulmonary sounds," *Bull. Eur. Physiopathol. Respir.*, vol. 23, pp. 265–270, 1987.

[12] H. Pasterkamp, R. E. Powell and I. Sanchez, "Lung sound spectra at standardized air flow in normal infants, children and adults," *Am. J. Respir. Crit. Care Med.*, vol. 154, pp. 424-430, 1996.

[13] V. Gross, A. Dittmar, T. Penzel, F. Schuttler and P. Von Wichert, "The relationship between normal lung sounds, age, and gender," *Am. J. Respir. Crit. Care Med.*, vol. 162, pp. 905-909, 2000.

[14] Y. L. Yap and Z. Moussavi, "Acoustic airflow estimation from tracheal sound power," *Proc. Canadian Conf. Elec. Comp. Eng.*, vol. 2, pp. 1073-1076, 2002.

[15] I. Hossain and Z. Moussavi, "Respiratory Airflow Estimation by Acoustical Means," *Proc. IEEE Eng. Med. Biol. Soci. (EMBS)*, vol. 2, pp. 1476 – 1477, 2002.

Formatted
Formatted
Formatted
Formatted
Formatted

[16] R. R. Coifman and M. V. Wickerhauser, "Adapted waveform 'de-noising' for medical signals and images," *IEEE Eng. Med. Biol. Mag.*, vol. 14:5, pp. 578-586, Sept./Oct. 1995.

[17] L. J. Hadjileontiadis and S. M. Panas, "A wavelet-based reduction of heart sound noise from lung sounds," *Int. J. Med. Infor.*, vol. 52, pp. 183-190, 1998.

[18] The American Lung Association website: http://www.lungusa.org/site/apps/s/content.asp?c=dvLUK9O0E&b=34706&content_id={D42B8CC3-A6E9-407F-8AD4-5F821C2E7FFE}

[19] J. Vanderschoot and H. J. W. Schreur, "Flow and volume related AR-modeling of lung sounds," *Proc. Ann. Int. Conf. IEEE Eng. Med. Biol. Soc.*, vol. 13:1, pp. 385-386, 1991.

[20] N. Gavriely, M. Nissan, A. H. E. Rubin and D. W. Cugell, "Spectral characteristics of chest wall breath sounds in normal subjects," *Thorax*, vol. 50, pp. 1292-1300, 1995.

[21] S. S. Kraman and P. M. Wang, "Airflow generated sound in a hollow canine airway cast," *Chest*, vol. 97, pp. 461-466, 1990.

[22] P. Leblanc, P. T. Macklem and W. R. Ross, "Breath sounds and distribution of pulmonary ventilation," *Am. Rev. Respir. Dis.*, vol. 102, pp. 10-16, 1970.

[23] Y. Ploysongsang, J. Dosman and P. T. Macklem, "Demonstration of regional phase differences in ventilation by breath sounds," *J. Appl. Physiol.*, vol. 46, pp. 361–368, 1979.

[24] S. S. Kraman and O. Austrheim, "Comparison of lung sound and transmitted sound amplitude in normal men," *Am. Rev. Respir. Dis.*, vol. 128, pp. 451-454, 1983.

[25] A. Pohlmann, S. Sehati and D. Young, "Effect of changes in lung volume on acoustic transmission through the human respiratory system," *Physiol. Meas.*, vol. 22, pp. 233-243, 2001.

[26] D. A. Rice, "Sound speed in pulmonary parenchyma," *J. Appl. Physiol.*, vol. 54, pp. 304–308, 1983.

[27] H. Pasterkamp, S. S. Kraman and G. R. Wodicka, "Respiratory sounds. Advances beyond the stethoscope," *Am. J. Respir., Crit. Care Med.*, vol. 156, pp. 974-987, 1997.

[28] N. Gavriely and D. W. Cugell, "Airflow effects on amplitude and spectral content of normal breath sounds," *J. Appl. Physiol.*, vol. 80, pp. 5-13, 1996.

[29] S. S. Kraman, "Effects of lung volume and airflow on the frequency spectrum of vesicular lung sounds," *Respir. Physiol.*, vol. 66, pp. 1-9, 1986.

[30] Z. Moussavi, M. T. Leopando, H. Pasterkamp and G. Rempel, "Computerized acoustical respiratory phase detection without airflow measurement," *Med. Biol. Eng. Comp.*, vol. 38(2), pp. 198-203, 2000.

[31] Guidelines for the diagnosis and management of asthma. National Heart, Lung and Blood Institute. National Asthma Education Program Expert Panel Report. *J. Allergy Clin. Immunol.,* vol. 88, pp. 425-434, 1991.

[32] M. Rossi, A. R. A. Sovijärvi, P. Piirilä, L. Vannuccini, F. Dalmasso and J. Vanderschoot, "Environmental and subject conditions and breathing maneuvers for respiratory sound recordings," *Eur. Respir. Rev.*, vol. 10:77, pp. 611-615, 2000.

[33] A. Suzuki , C. Sumi , K. Nakayama and M. Mori, "Real-time adaptive canceling of ambient noise in lung sound measurement," *Med. Biol. Eng. Comput.,* vol. 33: pp. 704–708. 1995.

[34] C. L. Que,, C. Kolmaga, L. G. Durand, S. M. Kelly and P. T. Macklem, "Phonospirometry for noninvasive measurement of ventilation: methodology and preliminary results," *J. Appl. Physiol.*, vol. 93, pp. 1515–1526, 2002.

[35] M. J. Mussell and Y. Miyamoto, "Comparison of normal respiratory sounds recorded from the chest and trachea at various respiratory airflow levels," *Front. Med. Biol. Eng.*, vol. 4(2), pp. 73-85, 1992.

[36] R. B Urquhart, J. Meghee and J. E. S. Macleod, "The diagnostic value of pulmonary sounds: a preliminary study by computer-aided analysis," *Comput. Biol. Med.*, vol. 11, pp. 129-139, 1981.

[37] E. F. Banaszak, R. C. Kory and G. L. Snider, "Phonopneumography," *Am. Rev. Respir. Dis.*, vol. 107, pp. 449-455, 1973.

[38] F. T. Wooten, W. W. Waring, M. J. Wegmann, W. F. Anderson and J. D. Conley, "Method of respiratory sound analysis," *Med. Instrum.*, vol. 12, pp. 254-257, 1978.

[39] R. Dosani and S. S. Kraman, "Lung sound intensity in normal man: a contour phonopneumographic study," *Chest*, vol. 4, pp. 628-631, 1983.

[40] S. S. Kraman, "The relationship between airflow and lung sound amplitude in normal subjects," *Chest*, vol. 86, pp. 225-229, 1984.

[41] B. E. Shykoff, Y. Ploysongsang, H. K. Chang, "Airflow and normal lung sounds," *Am. Rev. Respir. Dis.*, vol. 137, pp. 872-876, 1988.

[42] G. Charbonneau, M. Sudraud and G. Soufflet, "A method to evaluate flow rate from breath sounds," *Bull. Eur. Physiopathol. Respir.*, vol. 23, pp. 265-270, 1987.

[43] D. G. Tinkelman, C. Lutz and B. Conner, "Analysis of breath sounds in normal and asthmatic children and adults using computer digitized airway phonopneumography (CDAP)," *Respir. Med.*, vol. 85(2), pp. 125-131, 1991.

[44] L. Vannuccini, J. E. Earis, P. Helistö, B. M. G. Cheetham, M. Rossi, A. R. A. Sovijärvi and J. Vanderschoot, "Capturing and preprocessing of respiratory sounds," *Eur. Respir. Rev.*, vol.10:77, pp. 616-620, 2000.

[45] H. Pasterkamp, R. Fenton, A. Tal, and V. Chernick, "Interference of cardiovascular sounds with phonopneumography in children," *Am. Rev. Respir. Dis.* vol. 131, no. 1, pp. 61-64, 1985.

[46] V. K. Iyer, P. A. Ramamoorthy, H. Fan and Y. Ploysongsang, "Reduction of heart sounds from lung sounds by adaptive filtering," *IEEE Trans. Biomed. Eng.*, vol. 33(12), pp. 1141-1148, 1986.

[47] M. Kompis and E. Russi, "Adaptive heart sound reduction of lung sounds recorded by single microphone," *Proc. 14th Annu. Int. Conf. IEEE Eng. Med. Biol. Soc.*, vol. 33, pp. 1141-1148, 1986.

[48] L. Yip and Y. T. Zhang, "Reduction of heart sounds from lung sound recordings by automated gain control and adaptive filtering techniques," *Proc. 23rd Ann. Int. Conf. IEEE Engineering in Medicine Biology Society, EMBC'01*, Istanbul, Turkey, vol. 3, pp. 2154-2156, 2001.

[49] S. Charleston and M. R. Azimi-Sadjadi, "Reduced order Kalman filtering for the enhancement of respiratory sounds," *IEEE Trans. Biomed. Eng.*, vol. 43(4), pp. 421-424, 1996; Erratum in vol. 43(6), pp. 668, June 1996.

[50] Y.-S. Lu, W.-H. Liu and G.-X. Qin, "Removal of the heart sound noise from the breath sound," *Proc. 10th Ann. Int. Conf. IEEE Engineering in Medicine Biology Society, EMBC'88*, pp. 175-176, 1988.

[51] L. J. Hadjileontiadis and S. M. Panas, "Adaptive reduction of heart sounds from lung sounds using fourth-order statistics," *IEEE Trans. Biomed. Eng.*, vol. 44(7), pp. 642-648, 1997.

[52] S. Charleston, M. R. Azimi-Sadjadi and R. Gonzalez-Camarena, "Interference cancellation in respiratory sounds via a multiresolution joint time-delay and signal-estimation scheme," *IEEE Trans. Biomed. Eng.*, vol. 44(10), pp. 1006-1019, 1997.

[53] J. Gnitecki, Z. Moussavi and H. Pasterkamp, "Recursive least squares adaptive noise cancellation filtering for heart sound reduction in lung sound recordings," *Proc. 25th Ann. Int. Conf. IEEE Eng. Med. Biol. Soc., EMBS'03.*

[54] N. Gavriely, ed. With contribution by D. W. Cugell, Breath Sounds Methodology, Boca Raton, FL, CRC Press, ISBN: 0849355001, 1995.

[55] A. V. Oppenheim and R. W. Schafer, Discrete-Time Signal Processing, 2nd ed., Prentice-Hall, ISBN: 0137549202, 1999.

[56] The MathWorks Inc., Signal Processing Toolbox. Matlab function 'hilbert'. http://www.mathworks.com/access/helpdesk/help/toolbox/signal/functionlist.html

[57] O. Bratteli and P. Jorgenson, Wavelets Through a Looking Glass: The World of the Spectrum, Boston, MA: Birkhäuser, ISBN: 0817642803, 2002.

[58] S. G. Mallat, "A theory of multi-resolution signal decomposition: The wavelet representation," *IEEE Trans. Pattern Anal. Machine Intel.*, vol. 11:5, pp. 578-586, 1989.

[59] I. Daubechies, "Ten Lectures on Wavelets," *SIAM*, Philadelphia, 1992.

[60] D. L. Donoho, "De-noising by soft thresholding," *IEEE Trans. Inf. Theory*, vol. 41(3), pp. 613-627, 1995.

[61] D. L. Donoho and I. M. Johnstone, "Ideal spatial adaptation by wavelet shrinkage," *J. Am. Stat. Assoc.*, vol. 90:432, pp. 1200-1224, 1995.

[62] L. J. Hadjileontiadis and S. M. Panas, "Separation of discontinuous adventitious sound from vesicular sounds using a wavelet-based filter," *IEEE Trans. Biomed. Eng.*, vol. 44(12), pp. 1269-1281, 1997.

[63] I. Daubechies, "Orthonormal bases of compactly supported wavelets," *Commun. Pure. Appl. Math.*, vol. 41, pp. 909-996, 1988.

[64] P. M. Morse and K. U. Ingard, "Theoretical acoustics," *New York: McGraw-Hill*, pp. 761, 1968.

[65] L. P. Malmberg, A. R. Sovijärvi, E. Paajanen, P. Piirila, T. Haahtela and T. Katila, "Changes in frequency spectra of breath sounds during histamine challenge test in adult asthmatics and healthy control subjects," *Chest,* vol. 105, pp. 122-131, 1994.

[66] K. Anderson, S. Aitken, R. Carter, J. E. MacLeod and F. Moran, "Variation of breath sound and airway caliber induced by histamine challenge," *Am. Rev. Respir. Dis.*, vol. 141, pp. 1147-1150, 1990.

[67] H. Pasterkamp, R. Consunji-Araneta, Y. Oh and J. Holbrow, "Chest surface mapping of lung sounds during mathacholine challenge," *Pediatr. Pulmonol.*, vol. 23, pp. 21-30, 1997.

[68] S. Patel, S. Lu, P. Doerschuk and G. R. Wodicka "Sonic phase delay from trachea to chest wall: spatial and inhaled gas dependency," *Med. Biol. Eng., Comput.*, vol. 33, pp. 571-574, 1995.

[69] N. Gavriely, M. Nissan, D. Cugell and A. Rubin, "Respiratory health screening using pulmonary function tests and lung sound analysis," *Eur. Respir. J.*, vol. 7, pp. 35-42, 1994.